RESEARCH

Phylogenetic signal from rearrangements in 18 Anopheles species by joint scaffolding extant and ancestral genomes

Yoann Anselmetti[1,2], Wandrille Duchemin[2,3], Eric Tannier[2,3], Cedric Chauve[4] and Sèverine Bérard[1*]

*Correspondence: Severine.Berard@umontpellier.fr
[1]ISEM - Institut des Sciences de l'Évolution, UMR 5554, Université de Montpellier, CNRS, IRD, EPHE, Place Eugène Bataillon, 69622 Villeurbanne, France
Full list of author information is available at the end of the article
†Equal contributor

Abstract

Genomes rearrangements carry valuable information for phylogenetic inference or the elucidation of molecular mechanisms of adaptation. However, the detection of genome rearrangements is often hampered by current deficiencies in data and methods: Genomes obtained from short sequence reads have generally very fragmented assemblies, and comparing multiple gene orders generally leads to computationally intractable algorithmic questions. We present a computational method, ADSEQ, which, by combining ancestral gene order reconstruction, comparative scaffolding and *de novo* scaffolding methods, overcomes these two caveats. ADSEQ provides simultaneously improved assemblies and ancestral genomes, with statistical supports on all local features. Compared to previous comparative methods, it runs in polynomial time, it samples solutions in a probabilistic space, and it can handle a significantly larger gene complement from the considered extant genomes, with complex histories including gene duplications and losses. We use ADSEQ to provide improved assemblies and a genome history made of duplications, losses, gene translocations, rearrangements, of 18 complete *Anopheles* genomes, including several important malaria vectors. We demonstrate the method's ability to improve extant assemblies accurately through a procedure simulating realistic assembly fragmentation. We study a debated issue regarding the phylogeny of the *Gambiae complex* group of *Anopheles* genomes in the light of the evolution of chromosomal rearrangements, suggesting that the phylogenetic signal they carry can differ from the phylogenetic signal carried by gene sequences, more prone to introgression. We also provide additional support for a differentiated mode of evolution of the sex chromosome and of the autosomes in these mosquito genomes.

Keywords: Scaffolding; Comparative genomics; Mosquito genomics

Introduction

The promises of using genes as evolutionary markers for phylogeny, introduced half a century ago by Zuckerkandl and Pauling [1], have been largely deluded so far [2,3]. At every scale of evolution, gene histories can differ from organisms tree-like phylogeny due to non-tree like evolutionary mechanisms such as incomplete lineage sorting, horizontal gene transfer, hybridization, symbiosis, among others. This happens for example in the *Gambiae complex*, composed of several African *Anopheles* mosquito species, whose phylogeny is important to shed light on the origin of malaria transmission to humans [4], but is difficult to trace because of apparent extensive gene introgression within this complex [5,6]. Chromosomal rearrangements have been recognized, for an even longer time [7], as valuable phylogenetic markers, due to several reasons, including their lower occurrence rate compared to sequence evolution. They have proved to be of great interest for understanding mosquito evolution for example [8, 9], due to the fact introgression of whole chromosomes is much less frequent than introgression of genes [10]. Moreover, in terms of functional and ecological implications, chromosomal rearrangements have also been shown to be involved in important adaptation processes [11–13].

However chromosome evolution is still challenging to study, especially from short reads sequence data, and current methods have severe limitations that we outline now. First, some methods are limited to consider only chromosomal regions which are highly similar and whose differences are detected by genetic mapping, polytene chromosome banding, *in situ* hybridization or targeted sequencing [8]. Among methods which can handle whole genome sequence data [14–19], some consider only a small number of markers (often genes) with simple evolutionary histories (typically duplication-free histories and one-to-one orthologous gene families), and most of them require fully assembled extant genomes, aside of the recently published method DESCHRAMBLER [20]. As a consequence existing methods are hardly applicable to currently available genomic data, characterized by very short sequencing reads that can not resolve genomic repeats [21, 22], leading to highly fragmented genome assemblies, often in the form of hundred or thousands of contigs or scaffolds, where evolutionary breakpoints can not be distinguished from assembly artifacts.

Various types of data can help to improve the contiguity of genome assemblies obtained from short reads. For example Third-Generation Sequencing (TGS) technologies generate long, albeit noisy, sequencing reads that can resolve ambiguities due to repeats [23]; alternatively, chromosome conformation capture technologies [24, 25] or genome maps [26–28] have also been used successfully for scaffolding large genomes. However in the absence of long range sequence data or genome maps, the most widely used approach to scaffold contigs is the comparative approach, using one or several related genomes to guide the scaffolding. The principle of comparative scaffolding is to align contigs of a fragmented genome assembly onto one, or a set of, assembled reference genome(s) and to deduce contig adjacencies from the contiguity of the corresponding alignments along the reference(s). Most comparative scaffolding methods rely on a single reference genome, assumed to be closely related enough that contiguity along the reference can confidently imply contiguity in the newly assembled genome [29–35]. Such methods have mostly been used to assemble pathogen genomes using closely related assembled references, but have also be shown to be applicable in wider contexts, such as scaffolding an antelope genome using a cow genome as reference [34]. There exists few methods that can handle several reference genomes at once, that can be distinguished between methods that do require that the phylogenetic relation between the considered genomes are provided [36–39] and methods that do not need such information [40]. Moreover, only two methods make use of sequencing data that might not appear in the contigs to be scaffolded but can provide a valuable scaffolding signal that complements the comparative signal [35, 37]. All such methods are also limited to handle contigs containing repeats and discard repeated contigs.

An important feature of most of these methods is that they assume a hypothesis of genome rearrangement parsimony or near-parsimony to transfer contiguity information from the reference(s) to the genome of interest, this hypothesis being either explicit [30, 31, 33, 38] or implicit [36, 39]. This points at the fact that the comparative approach is a kind of conundrum: to scaffold genomes, comparative methods rely, at least implicitly, on a framework to compare genomes and detect conserved synteny and chromosomal rearrangements, while whole genome evolution methods do not fare well when provided with fragmented genome assemblies.

We introduce a new computational method, ADseq, that addresses the issues raised above, regarding both genome evolution by rearrangements and comparative genome scaffolding; we apply it to simultaneously study the chromosome evolution and improve the scaffolding of 18 *Anopheles* genomes, 16 of them recently sequenced by Neafsey *et al.* [4], including several important malaria vector species. The method ADseq does not need a fully assembled reference genome, as is required by most comparative scaffolding methods, but takes as input a set, that can be arbitrarily large, of fragmented genome assemblies, together with a species phylogeny. It also takes advantage of sequencing data such as paired-end reads, for species for which it is available. From this input, ADseq computes ancestral genome segments, as well as extant scaffolding adjacencies. Additionally, ADseq allows the user to infer evolutionary scenarios in terms of gene duplication, gene loss, gene displacement and genome rearrangement along each branch of the species phylogeny. A Gibbs-Boltzmann probabilistic framework based on the cost of adjacencies gain and breaks in evolutionary scenarios provides a statistical support on all ancestral and extant inferred adjacencies, with sequencing data used to define a prior on extant gene adjacencies. To handle genes whose history involves duplication and loss, ADseq relies on the use of reconciled gene trees, in terms of gene duplication and losses, which allows to use a much larger gene set than existing comparative scaffolding methods relying on one-to-one orthologous genes or gene families with simple duplication/loss histories. We present, together with the ADseq method, a validation procedure for the extant genome scaffolding aspect of ADseq relying on a realistic framework to generate artificially fragmented genome assemblies.

Using ADseq, we provide an analysis of whole genome evolution in a large set of *Anopheles* species with an unprecedented precision, being able to quantify duplications, losses, gene displacements between chromosomes, and chromosomal rearrangements. We work at a much finer scale than cytogenetics methods [41–47], rely on a larger gene complement than traditional genome rearrangement methods based on rothologous genes, and we provide a refined evolutionary analysis compared to [4] due to the improvement of extant genome scaffolding. In particular we find that gene displacements between chromosomes are much more frequent for genes belonging to families with duplication/loss histories, that previous studies handling only one-to-one orthologous genes had mostly outlooked. We also use our method to compare two alternative *Anopheles* phylogenies. We find that *Anopheles* genomes are compartmentalized between autosomes and sex chromosome according to duplications and chromosomal rearrangements, just as they were found to be according to gene sequences. We provide an alternative hypothesis to the conclusions of Fontaine *et al.* [5] about introgression of the major part of the genome. Indeed our measures of rearrangements and duplications are in favour of the phylogeny supported by most genes.

Materials and methods

We first describe the main methodological contribution of our work, the ADseq tool, followed by its application to the specific *Anopheles* genomes data set we analyze in detail. We begin by introducing some simple but important terminology. A gene, extant or ancestral, is seen as a directed DNA segment with two *extremities*. Genes are parts of larger segments containing one or several genes, which are contig, super-contigs, scaffolds or even chromosomes for well assembled genomes. Two genes that are contiguous along such a segment define an *adjacency* between one extremity of each gene, that we call a *gene adjacency*. Thus *segments of genes*, either extant or ancestral, are encoded by linearly organized sets of gene adjacencies. For extant genomes, such segments, corresponding to contigs, scaffolds or chromosomes, are observed, while for ancestral genomes, segments are reconstructed and are to be considered as hypothetical as they are not directly supported by sequence data. Ancestral segments have previously been termed Contiguous Ancestral Regions (CARs) [19, 48, 49]. However, to stress the similarity between scaffold in extant genomes and CAR in ancestral genome, we use the generic terminology ”segment” for both throughout this paper.

Assembly Recovery through Detection of Coevolution with sequencing data (ADseq)

ADseq builds upon a family of methods aimed at reconstructing the evolutionary history of gene adjacencies introduced with the DeCo algorithm [50] and extended along several lines in [51,52]. It is implemented within the package DeCoSTAR [53]. The aim of ADseq is to jointly scaffold extant genomes and reconstruct ancestral gene orders, through the joint analysis of phylogenomics and sequencing data.

ADseq takes as minimal input a species tree and a set of extant genomes data:gene adjacencies, homologous gene families and their associated reconciled gene trees (see for example [54] for background on reconciled gene trees). Reconciled gene trees implicitly yield the gene content of ancestral genomes. A key feature of ADseq is that the extant gene adjacencies can originate from genomes in various state of assembly, from fully assembled genomes —where gene adjacencies encode the gene order along the chromosomes—, to ambiguously assembled genomes represented as scaffolding graphs, through fragmented genomes assembled into contigs or scaffolds. Each extant gene adjacency is assigned a *prior* score in $[0, 1]$, expected to represent the confidence that the adjacency actually occurs in the genome of interest. This prior can be obtained from sequencing data or genome maps for example; so adjacencies between genes in fully assembled genomes will have a high prior score, while a potential gene adjacency in a poorly assembled genome and that is not supported by a strong signal in terms of sequencing data will likely be assigned a low prior score.

ADseq processes independently all pairs of gene families for which at least one extant adjacency is observed between genes from these families. A *solution* of ADseq on such an instance is a set of extant and ancestral gene adjacencies between extant and ancestral genes of the two considered families, that are consistent with the given reconciled gene trees. Taking the obtained solutions over all pairs of gene families defining ADseq instances, ancestral adjacencies link ancestral genes extremities into ancestral genome segments, while extant adjacencies improve the scaffolding of the provided extant genomes and reduce their fragmentation. This, together with

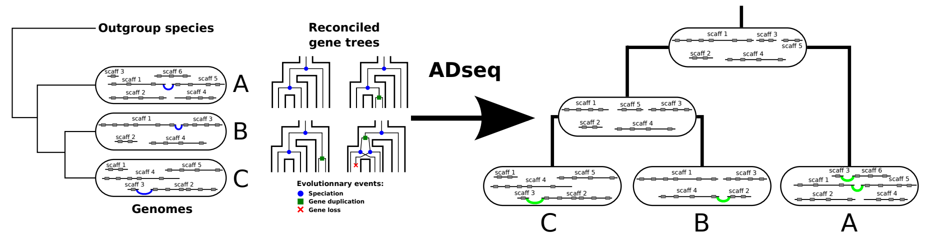

Figure 1 Input and output of ADseq. (Left) Input data: (1) a species tree with extant genomes (A, B and C) containing observed adjacencies (**black link**) and scaffolding gene adjacencies with a *prior* score (**blue link**); each grey box represents a gene. (2) reconciled gene trees representing evolutionary histories of gene families annotated by evolutionary events. (Right) Typical output: gene order across ancestral and extant genomes including new extant gene adjacencies with a *posterior* score (**green link**) between genes located at fragments extremities in the initial genome assemblies.

the reconciled gene trees, in turn provides an important input material for studying whole-genome evolution through mechanisms such as gene duplication, loss and transfer, introgression, or genome rearrangement. Figure 1 provides a high-level overview of the ADseq algorithm.

An important feature of ADseq is that, for each considered instance, it does not compute a single solution, but samples solutions from the, often large, associated search space. In order to sample solutions, ADseq relies on a *score*, function of the number of evolutionary events and the prior score of adjacencies. Any solution indeed yields a number of gains and breakages of gene adjacencies, that model genome rearrangement events consistent with the provided reconciled gene trees (see a description of the propagation rules that allow to infer gains/breakages from reconciled gene trees in the DeCo algorithm [50]). The *score* of a solution S is defined as $n(S) = g(S) + b(S) + c(S)$ where $g(S)$ is the number of gene adjacency gains scaled according to a user-defined unit cost of a gain; $b(S)$ is the number of gene adjacency breakages again scaled according to a user-defined unit cost; $c(S)$ is the cost of including or discarding extant adjacencies, based on their prior score: for an adjacency of *prior* score p, including the adjacency in a solution costs $-kT_0 \log(p)$ while discarding it from the solution costs $-kT_0 \log(1-p)$, where kT_0 is a pseudo-temperature that we discuss in details in Supplementary text.

A polynomial time and space Dynamic Programming (DP) algorithm samples solutions for a given instance with a probability proportional to their score. More precisely, ADseq can sample solutions under a Gibbs-Boltzmann probability distribution defined as follows: the Gibbs-Boltzmann score of a solution S is equal to $exp^{-n(S)/kT}$, where kT is a user-defined pseudo-temperature, and this score defines implicitly a probability distribution over the set of all solutions. Tuning the pseudo-temperature kT provides a control over the probability to sample parsimonious solutions: a low pseudo-temperature tends to increase the probability to sample most parsimonious solutions while a large pseudo-temperature skews the Gibbs-Boltzmann distribution toward the uniform distribution over the set of all solutions (we refer to [51] for more details on the Gibbs-Boltzmann framework applied to the DeCo algorithm).

In the present work, the *prior* scores of extant adjacencies are either 1.0 for adjacencies that are observed in a contig or scaffold, or a scaffolding score obtained from sequencing data using the scaffolding software BESST. Pairs of genes located at the extremities of contigs and for which sequencing data do not provide any evidence for a scaffolding adjacency receive a small prior score as described in [52] (see also Supplementary text). The *posterior* scores are defined as the frequency out of a sample of 100 solutions with temperatures $kT = kT_0 = 0.1$ that skews the Gibbs-Boltzmann distribution toward optimal solutions.

Linearization of extant and ancestral components.

After ADSEQ is applied to all considered pairs of gene families, the obtained result is a set of ancestral and extant gene adjacencies, each adjacency being assigned a *posterior* score. False positives – *i.e.* pairs of genes predicted inaccurately to be contiguous in an extant or ancestral genome–, can be due to errors in the data (for example errors in gene families or reconciled gene trees) or to errors in the inference process (for example the parsimony assumption might be wrong for some gene adjacencies). As a result, it is possible that a given gene (or gene extremity) belongs to more than two (more than one) adjacencies, which is incompatible with the expected linear structure of chromosomes.

To address this issue, we process the set of ADSEQ ancestral and extant adjacencies in such a way that they define linear ancestral and extant segments. To do so, we apply, independently for each species, a method used both in ancestral genome reconstruction [55] and scaffolding algorithms [56]. It consists in extracting, for each species, a Maximum-Weight Matching (MWM) in the graph whose vertices are gene extremities and edges are gene adjacencies, weighted by their posterior score. This MWM can still include circular segments, that are linearized by removing the least-weight edge of each such circular segment. Moreover, prior to this linearization step, we discard adjacencies whose posterior score is below a user-defined threshold, that was set to 0.1 after simulations aimed at measuring the accuracy of the ADSEQ algorithm (see Fig. 2). This linearization step is done independently for each species, ancestral or extant.

Application to the *Anopheles* data set

We now describe how we generated the data for the 18 *Anopheles* genomes.

Species trees.

The main species phylogeny we considered was taken from [5]. We call it the ”X phylogeny” as it is based on the X chromosome genes. It is the species tree used by default unless another is specified. We also considered an alternative ”WG phylogeny”, that was introduced in [5] as the most frequently observed among trees built using sequences from the autosomes (Fig. 4).

Genomic data.

Most genomic data we used were produced by the *A. 16 Genomes project* described in [4] and retrieved from VectorBase (`https://www.vectorbase.org`): genome assemblies (contigs, scaffolds, or chromosome arms), gene annotations, and gene sequences (CDS). For 16 out of the 18 considered *Anopheles* species, we retrieved from the NCBI Sequence Read Archive (SRA) paired-end Illumina libraries with an insert size of 180bp ('fragment' libraries) and mate-pair libraries with an insert size of 1.5kbp ('jump' libraries), both obtained from a single female individual. Additional low-coverage long-range sequencing libraries ('Fosill' libraries) were obtained from pools of individuals. Details are available in Tab. 2.

Gene families and trees.
We retrieved homologous gene families from orthologous gene groups of 21 *Culicidae* species recovered from the OrthoDBmoz2 database (`http://cegg.unige.ch/orthodbmoz2`) generated using OrthoDB [57]. We generated a multiple sequence alignment for each family, used RAxML [58] to compute draft gene trees with bootstrap supports, and then corrected these draft gene trees using ProfileNJ [59]. ProfileNJ contracts branches with low bootstrap support and, using the species tree, resolves the polytomies in a way that minimizes the number of duplications and losses in a reconciliation. This resulted in 14,940 gene trees containing 183,680 genes. We refer to Supplementary text and Figs. 5, 8, and 7, for a description of our preprocessing of these gene families, a comparison of the newly inferred gene trees with the original ones computed by the *Anopheles* consortium and for statistics on the inferred gene duplications and losses in these gene trees. As a species phylogeny is required to reconcile gene trees, we repeated the process described above for both the X phylogeny and the WG phylogeny.

Extant adjacencies and prior scores from sequencing data.
Sequencing reads from all libraries were filtered to discard low quality reads and trimmed to 75bp length using Trimmomatic [60], then mapped onto the contigs or scaffolds of the considered species using Bowtie2 [61]; for reads with multiple mappings, all of them were conserved. The scaffolding software BESST [62, 63] was then used to detect potential scaffolding adjacencies between pairs of contigs containing at least one annotated gene. Scaffolding adjacencies that were not supported by at least four pairs of reads were discarded. For remaining scaffolding adjacencies, we assigned a score defined as the arithmetic mean of the two scores computed by BESST, the link variation score and the link dispersity score. Detailed statistics on the scaffolding adjacencies so obtained are available in Fig. 10 and 11.

Genome fragmentation simulations for measuring the accuracy of ADseq for extant scaffolding

We developed a validation protocol of ADseq to measure its ability to propose reliable extant scaffolding adjacencies (see Fig. 12 for an illustration of the protocol). The key element is to provide to ADseq a genome whose assembly is more fragmented than the reference assembly, in order to verify that ADseq can retrieve the lost adjacencies. Moreover our simulation framework aims at generating a realistic fragmentation, as relying on a random fragmentation, as used in other validation protocols [16,52], generates data that are in general easy to scaffold using comparative methods.

To avoid this pitfall we simulated a fragmented assembly by re-assembling the considered genomes using KmerGenie [64] and Minia [65]. Minia was chosen due to its stringency in handling repeats, that leads to more conservative and fragmented assembly compared to other contig assemblers. We applied this protocol to a randomly chosen either all or half of the raw sequence reads, independently three times, with the species *A. albimanus*, *A. arabiensis* and *A. dirus*, whose positions in the species tree allow to consider various evolutionary contexts.

We ran ADseq as described above on these new assemblies and compared its results (scaffolding adjacencies) with the reference assemblies. We call a True Positive (TP) adjacency an adjacency inferred by ADseq and present in the initial genome assembly. A False Positive (FP) adjacency corresponds to an adjacency inferred by ADseq and not present in the reference genome assembly. A FP can however be a true adjacency not found by the reference assembly (*e.g.*, connecting two scaffolds), so we call Certain False Positive (CFP) a FP adjacency which extremities are not scaffold or contig extremities in initial genome assembly. Finally a False Negative (FN) is a pair of gene extremities that are contiguous in the initial assembly but are not inferred as an adjacency by ADseq. From these values we compute the usual *precision* and *recall* statistics, but using CFP for the false positives count.

Gene order evolution analysis

Assignment of chromosome segments.

To compare the evolution of *Anopheles* chromosomes, especially the apparent differences between the X chromosome and the autosomes described in [4], it is necessary to assign extant and ancestral chromosome segments to either the X chromosome or the autosomes. As *A. gambiae* is the only fully assembled genome in our data set, this is also the only genome for which such information is readily available; in all other species the genomes are assembled into scaffolds with no indication of whether this scaffold belongs to the X chromosome or an autosome, unless additional data is available, such as genome maps. We assigned extant and ancestral genes and segments to the X chromosome or autosomes using the following probabilistic method. For each gene g (ancestral or extant), a set of *An. gambiae* orthologs is defined as all *An. gambiae* genes from the same gene family than g whose last common ancestor with g in the reconciled gene tree is a speciation node. Note that this set might be empty, and that this definition includes the case where g is an ancestor of a *An. gambiae* gene. The probability of g being on the X chromosome is then defined as the frequency of orthologs located onto *An. gambiae* X chromosome, or, if no ortholog is present on this X chromosome, by a background probability, defined as the global frequency of *An. gambiae* genes on the X chromosome. Then each segment is given a probability to be located on the X chromosome as the mean of probabilities for all genes it contains. Each gene then inherits the probability of being on the X chromosome from the segment it belongs to.

Very recently an assignment of *An. albimanus* genes to chromosomes was published together with a new assembly [66] that we could use to verify that our assignment method is accurate: out of 8,840 genes assigned to a chromosome in the novel assembly, we correctly predicted the autosomal/X placement of 8,837 genes (comparing the assignment of higher probability and the assignment in the new assembly).

Gene movements (translocations).

For every couple of genes for which one is a direct descendant of the other, we inferred a gene movement (between the X chromosome and an autosome) if the probability of the ancestral gene being on the X chromosome is ≤ 0.2 while the probability of the descendant gene being on the X chromosome is ≥ 0.8, or conversely.

Detecting chromosomal rearrangements.
For every branch of the species tree, genes with exactly one exemplar in their family both in the ancestor and descendant species were selected. Then conserved adjacencies were computed, which are adjacencies present between ancestral genes and descendant homologous genes. In order to discard gene displacements, which are counted elsewhere, we filtered also genes which are not involved in any common adjacency. A *rearrangement* (gain or breakage of a gene adjacency) is counted every time two gene extremities are contiguous on a segment (with respect to the reduced selected set of genes) of the ancestor, but not on the descendant, or conversely. When they are not contiguous, in order to detect a certain genome rearrangement, we require also that they are not both the extremities of their segments, to avoid counting as a rearrangement a potentially undetected scaffolding adjacency. Rearrangements were not directly counted as gains and breakages output from ADSEQ because this count can be blurred by adjacencies gained or broken by gene duplications and gene losses. As a consequence, gene duplications and losses are not counted as rearrangements, that are limited to synteny breakages due to balanced rearrangements (inversions, transpositions, large translocations), that do not change the gene content.

We stress that this method to detect genome rearrangements is conservative and underestimates rearrangement counts, as it does not detect the rearrangements hidden by the assembly fragmentation of the considered genomes. Moreover, this underestimation can be biased by the degree of fragmentation of the compared species, so two numbers of rearrangements are not necessarily comparable in biological terms, even for species closely located in the species phylogeny. However, given the same genomes in the input, the numbers of rearrangements for two different phylogenies are comparable, as are the number of rearrangements in sex chromosomes and autosomes.

Data accessibility

Data used in this study are available on the github repository: https://github.com/YoannAnselmetti/DATA_Phylogenetic-signal-from-rearrangements-in-18-Anopheles-species.

Results

The results are organized in three parts. First, we describe the results of the simulation-based evaluation of the accuracy of ADSEQ to recover extant scaffolding adjacencies. Then we describe extant and ancestral genomes obtained with ADSEQ, and analyze important aspects of their evolutionary history. Finally we use ADSEQ to evaluate different species trees and re-examine the conclusions of [5] regarding species evolution.

Validation of the ADSEQ algorithm for extant scaffolding

We compared the scaffolding performance of ADSEQ with two other methods, on the same data set of realistically fragmented genomes (see Methods). One is using

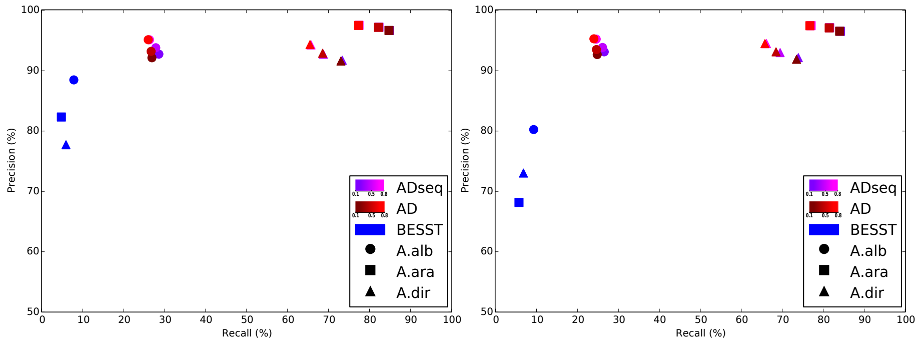

Figure 2 Precision and recall statistics for scaffolding adjacencies on three artificially fragmented genomes (A.alb: A. albimanus, A.ara: A. arabiensis and A.dir: A. dirus). Left graph: results with 50% of reads. **Right graph:** results with all reads. The different methods results are plotted with the precision on the Y axis and the recall on the X axis. For ADSEQ and AD, results for three different adjacency support thresholds (0.1, 0.5 and 0.8) before genome linearization are plotted and represented with a color gradient. Note: A True Positive (TP) adjacency requires the proper orientation of both genes.

sequence information only, BESST [63], while the other one is using the comparative approach only, on the same phylogenomic data, AD (ADSEQ, where the possibility of using sequence information is turned off). Figure 2 shows the precision statistic in function of the recall statistic for the two data sets (sampling 50% of the reads or using them all). For ADSEQ and AD, different values of the threshold for filtering adjacencies prior to linearization (see Methods) were tested.

ADSEQ outperforms BESST in precision and recall independently of the threshold. This shows that in the majority of cases, adding phylogenomic information improves the recall without affecting the precision compared to a method purely based on sequence data. Additional results, where the gene orientation is not considered to determine an inferred adjacency as TP, are provided in Fig. 13. These results show that BESST has an equivalent precision and recall statistics compared to results of Fig. 2 where gene orientation is considered. This comparison shows that for most of inferred adjacencies the three methods inferred the right orientation for both genes involved in adjacency. In summary the combined approach using comparative signal and sequence data (ADSEQ) is giving significantly better results than a method based on sequence alone (BESST).

We now compare ADSEQ and AD. Precision and recall statistics are slightly better with ADSEQ than with AD for all considered threshold values (except for *A. dirus* for a threshold of 0.5 where precision is slightly better for AD than ADSEQ). For *A. albimanus*, with all reads considered, ADSEQ outperforms AD for recall statistic for a threshold fixed to 0.1 and 0.5. So from a quantitative point of view, adding sequence data seems to have a smaller impact on the recall and precision statistics compared to using synteny evolution. Note however that the combination of both supports for extant scaffolding adjacencies (sequence data and synteny evolution) is an important by-product of ADSEQ. A phylogenetic method alone is more difficult to trust in the absence of sequence data. So even if the general statistics are comparable, the additional support brought by the sequence data is an important feature. Moreover, additional results in Figs. 16 and 17 strongly support that a joint combination of phylogenetic and sequence signals (ADSEQ)

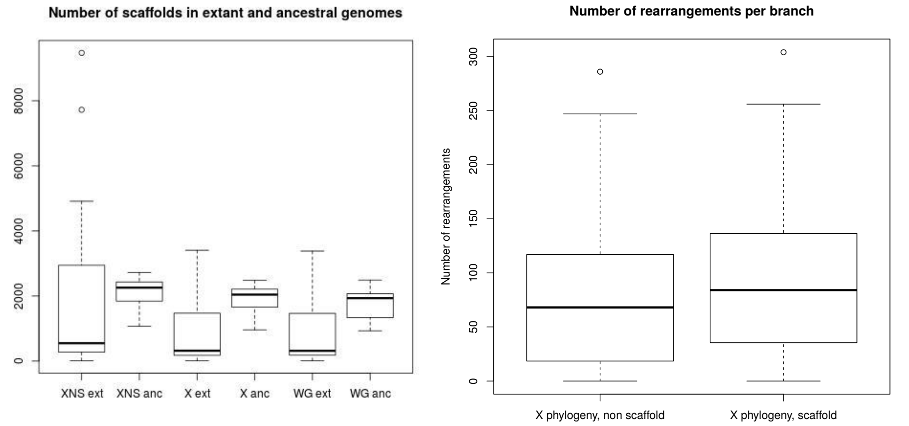

Figure 3 Left: Number of segments in extant and ancestral genomes, according to three runs of ADseq in three different conditions. In the first run, we turn off the scaffolding mode on the X phylogeny, that is, it only constructs ancestral segments. The first column "XNS ext" thus describes the initial assembly, and "XNS anc" the assembly of ancestral genomes when reconstructed without extant scaffolding. In the second and third runs, the scaffolding mode was turned on, and run with the X phylogeny ("X ext" and "X anc") and the WG phylogeny ("WG ext" and "WG anc"). **Right: Number of rearrangements over all branches of the X phylogeny, with and without the scaffolding mode.**

overpasses an *a posteriori* combination of phylogenetic signal and sequence data (AD + BESST) for scaffolding improvement. These results show indeed that combining AD + BESST slightly overpasses ADseq in term of recall statistic (stronger TP adjacencies) but at the expense of a strong decrease of the precision.

Improved scaffolding of *Anopheles* extant and ancestral genomes

Properties of the improved assemblies for *Anopheles* extant genomes and of the reconstructed *Anopheles* ancestral genomes segments are summarized in Fig. 3. We describe three runs of ADseq: one without proposing extant scaffolding adjacencies (which amounts to use the DeClone algorithm [51] to reconstruct ancestral genomes without improving extant genomes) and two with ADseq using the X and WG species phylogenies. The first observation that can be made is that the ability to create extant scaffolding adjacencies has a very significant impact on the ability to reconstruct ancestral segments, that define ancestral genomes at a similar level of fragmentation than the improved extant genomes. This effect is important toward refined genome evolution analysis that rely on the ancestral segments as input material, especially to detect chromosomal rearrangements.

Tab. 5 and Figs. 18, 19, and 20, provide more detailed illustration and statistics on the improved scaffolding. We observe that from 36,634 initial extant segments (contigs, supercontigs and scaffolds after the various filterings steps described in Methods and SI text), we scaffold the extant genomes into 13,525 segments, with an average number of 94 genes per segment up from 37 before running ADseq. Very similar results are obtained for all genomes independently of the chosen phylogeny, confirming the overall picture described in Fig. 3-Left.

On the right side of Fig. 3, we can observe that we retrieve a significantly (Wilcoxon paired test, p-value $< 10^{-4}$) higher number of rearrangements by the joint scaffolding technique than by just constructing ancestral genomes without scaffolding extant genomes. So the joint scaffolding of extant and ancestral genomes is beneficial to both. In particular scaffolding extant genomes while reconstructing ancestral genomes gives access to more information regarding the evolutionary history.

An interesting feature of ADseq is the possibility that the linearization step does delete an observed gene adjacency in an extant genome. This is unlikely as observed adjacencies have the highest score in the linearization procedure, but it can happen if it is in conflict with other adjacencies with high posterior probability. It happened only once in our dataset, for an adjacency between two *A. culcifacies* genes. The two genes were predicted in the reverse order, or equivalently in the reverse orientation, because all identified homologs were arranged similarly. This can be explained either by two inversions, one encompassing each gene, or by an assembly or annotation error. This shows that our approach can also detect questionable adjacencies in the given extant assemblies.

Evolution and phylogeny

ADseq is not a phylogenetic method *per se*, as it requires a given species phylogeny and does not include an extension to search an optimal phylogeny according to some evolutionary criterion. However as a method which infers ancestral gene orders and evolutionary events, and is computationally efficient (all steps that require a species phylogeny, including the correction of gene trees with ProfileNJ, the reconciliation of the gene trees with the species trees, and the joint scaffolding / ancestral genome reconstruction takes five hours on a laptop), it can be used to compare a few selected competing phylogenies. To this aim we compared several measures obtained by the same methods using the two phylogenies, WG and X, the later being shown in [5], to depict accurately the species evolution, following an argument based on the comparison of branch lengths of the gene trees.

Duplications.

Our pipeline using ProfileNJ to correct gene trees allows to record gene duplications. We counted a total of 6,461 duplications for the X phylogeny, against 6,159 duplications for the WG phylogeny (see Table 1). This means that for many gene families, a duplication was identified in the X phylogeny and not in the WG phylogeny. For these families, a well supported branch (100% bootstrap with RaxML) was compatible with the WG phylogeny but not with the WG phylogeny, indicating that well supported branches are more often compatible with the WG phylogeny. This supports the result of [5] that most genes follow the WG phylogeny. The fact that this is observed on the autosomes and not on the X phylogeny also supports that the genomes evolve with two compartments.

Scaffolding and ancestral genome reconstruction.

On the left side of Fig. 3, we can observe a first difference between the results obtained with the X and the WG phylogenies: the extant scaffolding is slightly better (in terms of fragmentation level of the extant genomes) with the X phylogeny (mean segment number is 835 genes for the X phylogeny, versus 840 for the WG phylogeny), while the ancestral scaffolding is better with the WG phylogeny (mean segment number is 1,860 for the X phylogeny, versus 1,756 for the WG phylogeny). The better extant scaffolding with the X phylogeny can be attributed to the basal position of the genome with best assembly (*A. gambiae*) in the *Gambiae complex*. Indeed in ADSEQ the sister species can be assembled according to *A. gambiae*, but outgroup species cannot, so the assembly is necessarily better if a fully assembled genome has more sisters species and less outgroups as it is the case with *A. gambiae* in the X phylogeny. Interestingly ancestral genomes are better scaffolded with the WG phylogeny, even with this sister-branch artifact that concerns extant genomes. This better ancestral genome reconstruction obtained with the WG phylogeny could be considered as a first signal contradicting the hypothesis that the X phylogeny is the true species phylogeny, although it does not allow to draw definitive conclusions.

Conflict.

With both phylogenies we also measured the level of syntenic conflicts, defined as the sum of the posterior scores of the adjacencies discarded during the linearization phase (data shown in SI text). We observe a higher level of syntenic conflicts in the X phylogeny (7,665) than in the WG phylogeny (6,319). According to simulations (described in SI text), the level of conflict is higher with a wrong phylogeny, even if it is not with the same order of magnitude than what we observe on our data. This could be seen as a second element contradicting the sequence-based hypothesis that the X phylogeny is the true species phylogeny, although the high level of conflict observed with both phylogenies here again does not allow to draw reliable conclusions.

Gene movements (translocations).

As it is believed there have been no large-scale rearrangement between the X chromosome and the autosomes in the *Anopheles* history [4, 67], we could assign most extant and ancestral segments (at least almost all that contain more than one gene) either to the X chromosome or to an autosome, with high accuracy (see Methods). Then we identified which genes moved from the X chromosome to an autosome, or conversely, by screening all couples of direct ancestor/descendant genes, one being in a segment assigned to the X chromosome and the other to an autosome. We found 429 genes having moved from the X chromosome to an autosome, and 469 from an autosome to the X chromosome, which confirms the trend found by Neafsey *et al.* [4] (59 over 132 gene movements originated from the X chromosome), although we draw our conclusion from experiments using now many more genes than in [4].

Genome rearrangements.

We now turn to detecting genome rearrangements, as defined in the Methods section. In particular, we stress that we look for breaks and gains of gener adjacencies due to genome rearrangements such as inversions, transpositions and translocations, excluding duplications and losses, as well as adjacency breaks and gains due to duplications and losses. Moreover, due to the fragmented nature of many ancestral genomes, we expect to underestimate the true number of synteny breaks and gains.

We detect 3,364 gains or breakages of adjacencies (860 in the *Gambiae complex*) using the X phylogeny, and 3,176 using the WG phylogeny (590 in the *Gambiae complex*). The difference is illustrated in Fig. 4. Between the two competing phylogenies,

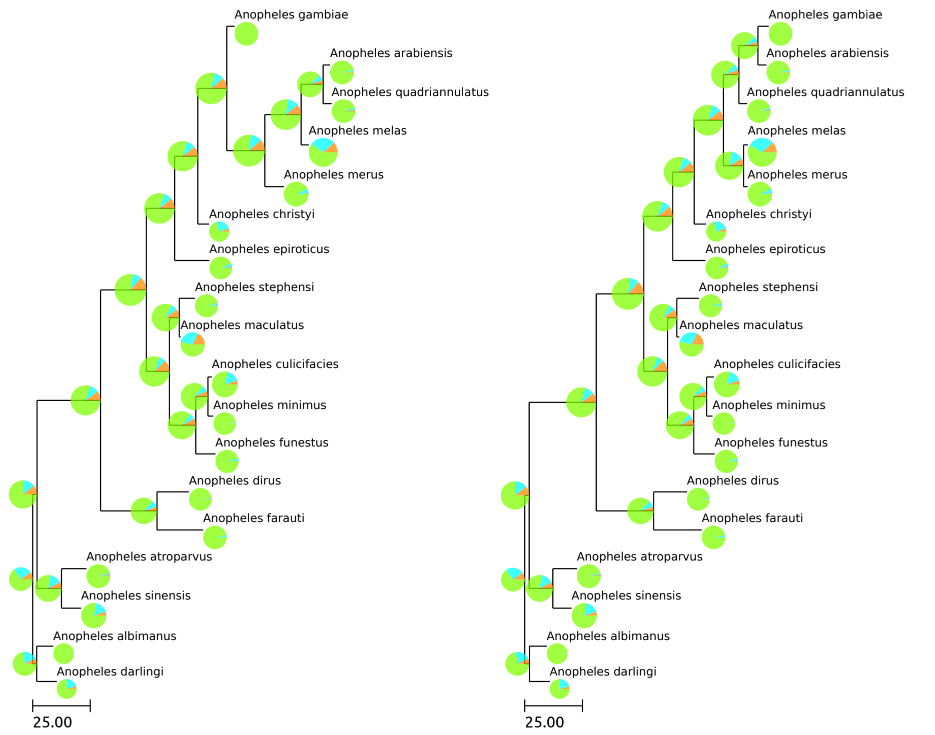

Figure 4 A. species trees (left: X phylogeny, right: WG phylogeny) with rearrangements per adjacency as branch lengths ($\times 10^{-3}$). The pie chart for a given species represents the adjacency degree of the genes of this species: orange represents genes with no adjacency, light blue genes with adjacency degree of 1 and green genes with adjacency degree of 2. Moreover, the diameter of each chart is proportional to the number of genes in the corresponding species.

one can observe a 30% decrease in the number of rearrangements within the *Gambiae complex* with the WG phylogeny compared to the X phylogeny. These gains/breaks of adjacencies can be combined along each branch to detect inversions, defined by pairs of breaks in the ancestor and pairs of gains in the descendant involving the same four gene extremities. This lead to the identification of 242 inversions in the X phylogeny (including 16 inversions in the *Gambiae complex*, including 4 on the single lineage to *A. gambiae*) and 240 inversions with the WG phylogeny, with only 4 in the *Gambiae complex*, two of them on the branch leading to *A. gambiae*.

Comparison of sex chromosomes and autosomes evolution.

Sex chromosome and autosomes have different evolutionary modes, according to duplications and rearrangements. Table 1 summarizes the number of inferred events of gene duplication and genome rearrangement in the sex chromosomes and autosomes, depending on the chosen phylogeny.

Event	X phylogeny		WG phylogeny	
	X chr.	Autosomes	X chr.	Autosomes
Duplications	604	5857	606	5553
Rearrangements	415	2949	416	2760

Table 1 Numbers of inferred rearrangements and duplications in the X chromosome and in the autosomes, according to the phylogeny (X or WG) used as a parameter of ADseq.

A striking observation is the different behavior of the X chromosome and of the autosomes regarding duplications and genome rearrangements. We do not count loss events to compare phylogenies because the absence of genes can be due to the fragmented assembly and not necessarily to actual gene losses during evolution. This compartmentalization was observed by [5] for genes and attributed to introgression in the autosomes; it was also noticed in [4] that the genome rearrangement rate was much higher in the X chromosome than in autosomes. We observe here a similar trend. We computed genome rearrangement rates by normalizing the number of observed gains and breaks of gene adjacencies by the number of gene adjacencies in the whole set of extant and ancestral genomes; with the X phylogeny we could observe that the X chromosome has a rearrangement rate equal to 1.46 times the rate observed in the autosomes, a figure that is similar (1.57) using the WG phylogeny. The observed higher reate of rearrangement in the X chromosome is in fact likely higher, as the relative fragmentation of the chromosome X is higher compared to the autosomes in most species both extant and ancestral (data not shown).

Moreover, we can observe interesting differences between the X and WG phylogenies. Constantly less events are found on the X chromosome with the X phylogeny, while less events are found on the autosomes with the WG phylogeny. It seems indeed that not only do genes follow different histories because of introgression [5], but also entire chromosomes do. However, the observed compartmentalization alone does not allow us to specify which part of the genome has followed the species diversification. As the *Gambiae complex* is estimated to be 2.2 million years old, it is reasonable to use parsimony arguments concerning rearrangements (see argument in the next paragraph). If we do so, we find less rearrangements in total in the WG phylogeny: even normalized by the number of adjacencies (because an increase in the number of rearrangements might be the effect of a higher number of adjacencies): $9.15\ 10^{-3}$ for the WG phylogeny versus $9.68\ 10^{-3}$ for the X phylogeny. This means that rearrangements do not yield the same phylogenetic signal than the one suggested in [5]), which puzzles the evolutionary scenario in the *Gambiae complex* [68].

Assessing the relevance of rearrangements parsimony.

The fact that parsimony can give a good account on the phylogeny can be questioned. Indeed, rearrangements in *Anopheles* are not uniformly distributed [69], they can show some degree of convergence, and rearrangements can show inter-species polymorphism. To test whether in the *Gambiae complex* we are in the domain of validity of parsimony, we compared the gene order of *A. gambiae* with *A. albimanus*, which, following the recent improved assembly of *A. albimanus*, are the two genomes which have their genes assigned to chromosomes. We selected all genes with an assignment to a chromosome, and applied the EM2 distance estimator [70]. It is based on a non uniform model of genome rearrangements which has proved to give the most reliable results on mammalian genomes, whose evolution spans a similar amount of time than the *Anopheles* genomes. We found an estimation of 1,313 inversions with the statistical estimator, while the parsimony solution was 1,300 (data not shown). So the parsimony result is within in the 1% interval of the statistical method, far from saturation. As *A. gambiae* and *A. albimanus* are separated by approximately 79 million years of evolution, we may suppose that, in the 2 or 3 million years that have shaped the *Gambiae complex*, rearrangements were not numerous enough to contradict parsimony.

Discussion

An important contribution of our work is the unification of two domains of research, namely genome scaffolding, and the evolution of gene order and ancestral genome reconstruction. They are usually separated despite the similarity of their objectives (reconstructing ancestral gene order is akin to a scaffolding procedure if ancestral genes are considered as contigs). Our work improves on previous works (especially [37, 39, 71]) in several aspects. In particular, we integrate elements coming from more traditional phylogenetic methods, such as gene trees and reconciliations, in order to be able to handle a large gene complement that includes gene families with complex evolutionary histories. Another important aspect of our work is the validation procedure of the scaffolding method. We propose a novel simulation procedure which takes real sequence data but lowers the coverage and rely on a conservative contigs assembler to obtain a realistic fragmentation. Using this validation method, we show that combining both sequence data and comparison with related genomes in a phylogenetic context produce better scaffolds, at least in the context of *Anopheles* genomes.

The benefit of the joint approach that considers in the same framework scaffolding extant genomes and reconstructing ancestral genomes is evident from both the improved extant genomes assemblies, where we reduce the fragmentation from roughly 36,000 segments to below 14,000 segments, and the detection of genome rearrangements, where we observe again a much better resolution of ancestral genomes. This allows us to detect a statistically significantly larger number of genome rearrangements that can not be confused with assembly artifacts. To the best of our knowledge, ADSEQ is currently the only method that can process such a data set with many genomes, most of them provided with fragmented assemblies, while using a large complement of gene families without being limited by the nature of the evolution of these families in terms of duplications and losses, and using also sequencing data. Regarding extant genomes scaffolding, the quality of our results depends of a set of factors, such as the quality of the initial extant assemblies and the position in the species phylogeny; we do not gain much for well assembled species such as *A. albimanus* which is almost an outgroup, while we refine very well the assembly of the genomes of species such as *A. minimus* or *A. dirus*. It is important to note that while we rely on sequencing data in the present work, other sources of data such as genome maps for example could be used to define a prior score for scaffolding assemblies. In terms of genome rearrangements, we likely underestimates their actual number due to the fragmentation of the reconstructed ancestral genomes. This is a consequence the very conservative approach we follow that detects only rearrangements for which there is a clear support. It remains to see if more realistic models of genome rearrangements that do not rely on reconstructed ancestral gene orders would be able to cope, in terms of computational complexity and of robustness of the detected rearrangements, with both the large number of species considered here and the level of fragmentation of the extant genomes assemblies. Nevertheless, the results we obtain support strongly the observation of [4] that the X chromosome evolves by genome rearrangements at a much higher rate than the autosomes.

Finally, our work opens the way to several research avenues. Generally, our general approach that relies on the joint analysis of sequencing data and the comparative approach to improve the quality of extant genome data could be extended to correct other types of errors that assembly breakpoints. To cite a specific example, it could be extended to account for the well known problem of unassembled genes [72], that create apparent gene loss and rearrangement breakpoints. Other avenues could include the development of metrics to compare alternative species phylogenies or the introduction in the evolutionary model of introgression events.

Competing interests

The authors declare that they have no competing interests.

Author's contributions

ET, CC and SB designed the study. YA and WD implemented the method. YA applied the method to data. ET, CC and SB analyzed the results. YA, AT, CC, SB wrote the manuscript. All authors read and approved the manuscript.

Acknowledgements

This work is funded by the Agence Nationale pour la Recherche, Ancestrome project ANR-10-BINF-01-01, the MITACS Globalink program and the Natural Sciences and Engineering Research Council of Canada (NSERC), Discovery Grant RGPIN-249834. Data computation and analyses benefited from the Compute Canada Western Canada Research Grid (Westgrid) and Montpellier Bioinformatics Biodiversity (MBB) platform services.

Author details

[1]ISEM - Institut des Sciences de l'Évolution, UMR 5554, Université de Montpellier, CNRS, IRD, EPHE, Place Eugène Bataillon, 69622 Villeurbanne, France. [2]LBBE - Laboratoire de Biométrie et Biologie Évolutive, UMR 5558 Université Lyon 1, CNRS, 43 Boulevard du 11 novembre 1918, 24105 Kiel, Germany. [3]INRIA Grenoble - Rhône-Alpes, 655 Avenue de l'Europe, 38330 Montbonnot-Saint-Martin, France. [4]Department of Mathematics, Simon Fraser University, 8888 University Drive, V5A1S6 Burnaby, BC, Canada.

References

1. Zuckerkandl E, Pauling L. Molecules as documents of evolutionary history. J Theor Biol. 1965 Mar;8(2):357–366.
2. Springer MS, Gatesy J. The gene tree delusion. Molecular Phylogenetics and Evolution. 2016 Jan;94:1–33.
3. Doolittle WF, Brunet TDP. What Is the Tree of Life? PLoS Genetics. 2016 Apr;12:e1005912.
4. Neafsey DE, Waterhouse RM, Abai MR, Aganezov SS, Alekseyev MA, Allen JE, et al. Mosquito genomics. Highly evolvable malaria vectors: the genomes of 16 Anopheles mosquitoes. Science. 2015 Jan;347(6217):1258522. Available from: http://dx.doi.org/10.1126/science.1258522.
5. Fontaine MC, Pease JB, Steele A, Waterhouse RM, Neafsey DE, Sharakhov IV, et al. Mosquito genomics. Extensive introgression in a malaria vector species complex revealed by phylogenomics. Science. 2015 Jan;347(6217):1258524. Available from: http://dx.doi.org/10.1126/science.1258524.
6. Wen D, Yu Y, Hahn MW, Nakhleh L. Reticulate evolutionary history and extensive introgression in mosquito species revealed by phylogenetic network analysis. Molecular Ecology. 2016 Jun;25:2361–2372.
7. Dobzhansky T, Sturtevant AH. Inversions in the Chromosomes of Drosophila Pseudoobscura. Genetics. 1938 Jan;23(1):28–64.
8. Kamali M, Xia A, Tu Z, Sharakhov IV. A new chromosomal phylogeny supports the repeated origin of vectorial capacity in malaria mosquitoes of the Anopheles gambiae complex. PLoS Pathogens. 2012;8:e1002960.
9. Sharakhov IV. Chromosome phylogenies of malaria mosquitoes. Tsitologiia. 2013;55:238–240.
10. della Torre A, Merzagora L, Powell JR, Coluzzi M. Selective introgression of paracentric inversions between two sibling species of the Anopheles gambiae complex. Genetics. 1997 May;146:239–244.
11. Ayala D, Ullastres A, González J. Adaptation through chromosomal inversions in Anopheles. Frontiers in Genetics. 2014;5:129.
12. Ayala D, Acevedo P, Pombi M, Dia I, Boccolini D, Costantini C, et al. Chromosome inversions and ecological plasticity in the main African malaria mosquitoes. Evolution. 2017;71(3):686–701.
13. Love RR, Steele AM, Coulibaly MB, Traore SF, Emrich SJ, Fontaine MC, et al. Chromosomal inversions and ecotypic differentiation in *Anopheles gambiae*: the perspective from whole-genome sequencing. Molecular Ecology. 2016;25(23):5889–5906.
14. Tang J, Moret BME. Scaling up accurate phylogenetic reconstruction from gene-order data. Bioinformatics. 2003;19 Suppl 1:i305–i312.
15. Larget B, Simon D, Kadane J. Bayesian phylogenetic inference from animal mitochondrial genome arrangements. Journal of the Royal Statistical Society: Series B. 2002;.
16. Avdeyev P, Jiang S, Jr SA, Hu F, Alekseyev MA. Reconstruction of Ancestral Genomes in Presence of Gene Gain and Loss. Journal of Computational Biology. 2016;23(3):150–164. Available from: http://dx.doi.org/10.1089/cmb.2015.0160.
17. Hu F, Lin Y, Tang J. MLGO: phylogeny reconstruction and ancestral inference from gene-order data. BMC Bioinformatics. 2014 Nov;15:354.
18. Zheng C, Sankoff D. On the PATHGROUPS approach to rapid small phylogeny. BMC Bioinformatics. 2011;12(S-1):S4. Available from: http://dx.doi.org/10.1186/1471-2105-12-S1-S4.

19. Jones BR, Rajaraman A, Tannier E, Chauve C. ANGES: reconstructing ANcestral GEnomeS maps. Bioinformatics. 2012;28(18):2388–2390. Available from: http://dx.doi.org/10.1093/bioinformatics/bts457.
20. Kim J, Farré M, Auvil L, Capitanu B, Larkin DM, Ma J, et al. Reconstruction and evolutionary history of eutherian chromosomes. Proceedings of the National Academy of Sciences. 2017;114(27):E5379–E5388. Available from: http://www.pnas.org/content/114/27/E5379.abstract.
21. Nagarajan N, Pop M. Sequence assembly demystified. Nature Reviews Genetics. 2013;14(3):157–167. Available from: http://dx.doi.org/10.1038/nrg3367.
22. Treangen TJ, Salzberg SL. Repetitive DNA and next-generation sequencing: computational challenges and solutions. Nature Reviews Genetics. 2011;13(1):36–46. Available from: http://dx.doi.org/10.1038/nrg3117.
23. Berlin K, Koren S, Chin CS, Drake JP, Landolin JM, Phillippy AM. Assembling large genomes with single-molecule sequencing and locality-sensitive hashing. Nature Biotechnology. 2015;33(6):623–630. Available from: http://dx.doi.org/10.1038/nbt.3238.
24. Dudchenko O, Batra SS, Omer AD, Nyquist SK, Hoeger M, Durand NC, et al. De novo assembly of the *Aedes aegypti* genome using Hi-C yields chromosome-length scaffolds. Science. 2017;Epub ahead of print, doi:10.1126/science.aal3327.
25. Putnam NH, O'Connell BL, Stites JC, Rice BJ, Blanchette M, Calef R, et al. Chromosome-scale shotgun assembly using an in vitro method for long-range linkage. Genome Research. 2016 03;26(3):342–350.
26. Lewin HA, Larkin DM, Pontius J, O'Brien SJ. Every genome sequence needs a good map. Genome Research. 2009;19(11):1925–1928. Available from: http://dx.doi.org/10.1101/gr.094557.109.
27. Tang H, Zhang X, Miao C, Zhang J, Ming R, Schnable JC, et al. ALLMAPS: robust scaffold ordering based on multiple maps. Genome Biology. 2015;16(1):3+. Available from: http://dx.doi.org/10.1186/s13059-014-0573-1.
28. Fierst JL. Using linkage maps to correct and scaffold de novo genome assemblies: methods, challenges, and computational tools. Frontiers in Genetics. 2015;6:220. Available from: http://journal.frontiersin.org/article/10.3389/fgene.2015.00220.
29. Assefa SA, Keane TM, Otto TD, Newbold C, Berriman M. ABACAS: algorithm-based automatic contiguation of assembled sequences. Bioinformatics. 2009;25(15):1968–1969. Available from: http://dx.doi.org/10.1093/bioinformatics/btp347.
30. Rissman AI, Mau B, Biehl BS, Darling AE, Glasner JD, Perna NT. Reordering contigs of draft genomes using the Mauve Aligner. Bioinformatics. 2009;25(16):2071–2073. Available from: http://dx.doi.org/10.1093/bioinformatics/btp356.
31. Dias Z, Dias U, Setubal JC. SIS: a program to generate draft genome sequence scaffolds for prokaryotes. BMC Bioinformatics. 2012;13:96. Available from: http://dx.doi.org/10.1186/1471-2105-13-96.
32. Bao E, Jiang T, Girke T. AlignGraph: algorithm for secondary *de novo* genome assembly guided by closely related references. Bioinformatics. 2014;30(12):319–328. Available from: http://dx.doi.org/10.1093/bioinformatics/btu291.
33. Lu CL, Chen K, Huang S, Chiu H. CAR: contig assembly of prokaryotic draft genomes using rearrangements. BMC Bioinformatics. 2014;15:381. Available from: http://dx.doi.org/10.1186/s12859-014-0381-3.
34. Tamazian G, Dobrynin P, Krasheninnikova K, Komissarov A, Koepfli KP, O'Brien SJ. Chromosomer: a reference-based genome arrangement tool for producing draft chromosome sequences. GigaScience. 2016;5(1):38.
35. Shaik S, Kumar N, Lankapalli AK, Tiwari SK, Baddam R, Ahmed N. Contig-Layout-Authenticator (CLA): A Combinatorial Approach to Ordering and Scaffolding of Bacterial Contigs for Comparative Genomics and Molecular Epidemiology. PLoS ONE. 2016;11(6):1–19. Available from: http://dx.doi.org/10.1371%2Fjournal.pone.0155459.
36. Husemann P, Stoye J. Phylogenetic comparative assembly. Algorithms for Molecular Biology. 2010;5:3. Available from: http://dx.doi.org/10.1186/1748-7188-5-3.
37. Kim J, Larkin DM, Cai Q, Asan, Zhang Y, Ge RL, et al. Reference-assisted chromosome assembly. Proceedings of the National Academy of Sciences. 2013;110(5):1785–1790. Available from: http://www.pnas.org/content/110/5/1785.abstract.
38. Kolmogorov M, Raney BJ, Paten B, Pham SK. Ragout - a reference-assisted assembly tool for bacterial genomes. Bioinformatics. 2014;30(12):302–309. Available from: http://dx.doi.org/10.1093/bioinformatics/btu280.
39. Aganezov S, Alekseyev MA. In: Bourgeois A, Skums P, Wan X, Zelikovsky A, editors. Multi-genome scaffold co-assembly based on the analysis of gene orders and genomic repeats. vol. 9683. Cham: Springer International Publishing; 2016. p. 237–249.
40. Bosi E, Donati B, Galardini M, Brunetti S, Sagot M, Liò P, et al. MeDuSa: a multi-draft based scaffolder. Bioinformatics. 2015;31(15):2443–2451. Available from: http://dx.doi.org/10.1093/bioinformatics/btv171.
41. Sharakhov IV, Serazin AC, Grushko OG, Dana A, Lobo N, Hillenmeyer ME, et al. Inversions and gene order shuffling in Anopheles gambiae and A. funestus. Science. 2002 Oct;298:182–185.
42. Wang-Sattler R, Blandin S, Ning Y, Blass C, Dolo G, Touré YT, et al. Mosaic genome architecture of the Anopheles gambiae species complex. PloS ONE, year = 2007, volume = 2, pages = e1249, month = nov, issn = 1932-6203, abstract = Attempts over the last three decades to reconstruct the phylogenetic history of the Anopheles gambiae species complex have been important for developing better strategies to control malaria transmission We used fingerprint genotyping data from 414 field-collected female mosquitoes at 42 microsatellite loci to infer the evolutionary relationships of four species in the A gambiae complex, the two major malaria vectors A gambiae sensu stricto (A gambiae ss) and A arabiensis, as well as two minor vectors, A merus and A melas We identify six taxonomic units, including a clear separation of West and East Africa A gambiae ss S molecular forms We show that the phylogenetic relationships vary widely between different genomic regions, thus demonstrating the mosaic nature of the genome of these species The two major malaria

vectors are closely related and closer to A merus than to A melas at the genome-wide level, which is also true if only autosomes are considered However, within the Xag inversion region of the X chromosome, the M and two S molecular forms are most similar to A merus Near the X centromere, outside the Xag region, the two S forms are highly dissimilar to the other taxa Furthermore, our data suggest that the centromeric region of chromosome 3 is a strong discriminator between the major and minor malaria vectors Although further studies are needed to elucidate the basis of the phylogenetic variation among the different regions of the genome, the preponderance of sympatric admixtures among taxa strongly favor introgression of different genomic regions between species, rather than lineage sorting of ancestral polymorphism, as a possible mechanism, chemicals = Genetic Markers, citation-subset = IM, completed = 2008-08-21, country = United States, created = 2007-11-28, doi = 101371/journalpone0001249, issn-linking = 1932-6203, issue = 11, keywords = Animals; Anopheles gambiae, classification, genetics; Biological Evolution; Chromosomes, Artificial, Bacterial; Female; Genetic Markers; Genetic Variation; Genome; Microsatellite Repeats, genetics; Mosaicism, nlm = PMC2082662, nlm-id = 101285081, owner = NLM, pmc = PMC2082662, pmid = 18043756, pubmodel = Electronic, pubstatus = epublish, revised = 2016-10-19,;.

43. Coluzzi M, Sabatini A, della Torre A, Di Deco MA, Petrarca V. A polytene chromosome analysis of the Anopheles gambiae species complex. Science. 2002 Nov;298:1415–1418.
44. Caccone A, Min GS, Powell JR. Multiple origins of cytologically identical chromosome inversions in the Anopheles gambiae complex. Genetics. 1998 Oct;150:807–814.
45. Gentile G, Slotman M, Ketmaier V, Powell JR, Caccone A. Attempts to molecularly distinguish cryptic taxa in Anopheles gambiae s.s. Insect Molecular Biology. 2001 Feb;10:25–32.
46. Mathiopoulos KD, della Torre A, Santolamazza F, Predazzi V, Petrarca V, Coluzzi M. Are chromosomal inversions induced by transposable elements? A paradigm from the malaria mosquito Anopheles gambiae. Parassitologia. 1999 Sep;41:119–123.
47. Appawu MA, Baffoe-Wilmot A, Afari EA, Nkrumah FK, Petrarca V. Species composition and inversion polymorphism of the Anopheles gambiae complex in some sites of Ghana, west Africa. Acta Tropica. 1994 Feb;56:15–23.
48. Ma J, Zhang L, Suh BB, Raney BJ, Burhans RC, Kent WJ, et al. Reconstructing contiguous regions of an ancestral genome. Genome Research. 2006;16(12):1557–1565.
49. Chauve C, Tannier E. A methodological framework for the reconstruction of contiguous regions of ancestral genomes and its application to mammalian genomes. PLoS Computational Biology. 2008;4(11):e1000234.
50. Bérard S, Gallien C, Boussau B, Szöllősi GJ, Daubin V, Tannier E. Evolution of gene neighborhoods within reconciled phylogenies. Bioinformatics. 2012 Sep;28(18):i382–i388. Available from: http://dx.doi.org/10.1093/bioinformatics/bts374.
51. Chauve C, Ponty Y, Zanetti JPP. Evolution of genes neighborhood within reconciled phylogenies: an ensemble approach. BMC Bioinformatics. 2015 Dec;16(Suppl 19):S6. Available from: https://hal.inria.fr/hal-01245495.
52. Anselmetti Y, Berry V, Chauve C, Chateau A, Tannier E, Bérard S. Ancestral gene synteny reconstruction improves extant species scaffolding. BMC Genomics. 2015;16(Suppl 10):S11. Available from: http://www.biomedcentral.com/1471-2164/16/S10/S11.
53. Duchemin W, Anselmetti Y, Patterson M, Ponty Y, Berard S, Chauve C, et al. DeCoSTAR: Reconstructing the ancestral organization of genes or genomes using reconciled phylogenies. Genome Biology and Evolution. 2017;Available from: http://pbil.univ-lyon1.fr/software/DeCoSTARhttps://academic.oup.com/gbe/article-lookup/doi/10.1093/gbe/evx069.
54. Jacox E, Chauve C, Szöllősi GJ, Ponty Y, Scornavacca C. ecceTERA: comprehensive gene tree-species tree reconciliation using parsimony. Bioinformatics. 2016 Feb;Available from: http://dx.doi.org/10.1093/bioinformatics/btw105.
55. Maňuch J, Patterson M, Wittler R, Chauve C, Tannier E. Linearization of ancestral multichromosomal genomes. BMC Bioinformatics. 2012;13 Suppl 19:S11.
56. Mandric I, Zelikovsky A. ScaffMatch: scaffolding algorithm based on maximum weight matching. Bioinformatics. 2015;31(16):2632–2638. Available from: http://dx.doi.org/10.1093/bioinformatics/btv211.
57. Kriventseva EV, Tegenfeldt F, Petty TJ, Waterhouse RM, Pozdnyakov IA, Ioannidis P, et al. OrthoDB v8 : update of the hierarchical catalog of orthologs and the underlying free software. Nucleic Acids Research. 2015;43(Database issue):250–256.
58. Stamatakis A. RAxML-VI-HPC: Maximum likelihood-based phylogenetic analysis with thousands of taxa and mixed models. Bioinformatics. 2006;22:2688-2690.
59. Noutahi E, Semeria M, Lafond M, Seguin J, Boussau B, Guéguen L, et al. PLoS ONE, number = 8, publisher = Public Library of Science, title = Efficient gene tree correction guided by genome evolution, volume = 11, year = 2016;.
60. Bolger AM, Lohse M, Usadel B. Trimmomatic: a flexible trimmer for Illumina sequence data. Bioinformatics. 2014;30:2114.
61. Langmead B, Salzberg SL. Fast gapped-read alignment with Bowtie 2. Nature Methods. 2012;9(4):357–359.
62. Sahlin K, Vezzi F, Nystedt B, Lundeberg J, Arvestad L. BESST - Efficient scaffolding of large fragmented assemblies. BMC Bioinformatics. 2014;15(1):281. Available from: http://www.biomedcentral.com/1471-2105/15/281.
63. Sahlin K, Chikhi R, Arvestad L, Science C. Genome scaffolding with PE-contaminated mate-pair libraries. bioRxiv preprint. 2015;p. 1–13. Available from: http://biorxiv.org/content/early/2015/08/28/025650.article-metrics.
64. Chikhi R, Medvedev P. Informed and automated *k*-mer size selection for genome assembly. Bioinformatics. 2014;30(1):31–37. Available from: http://dx.doi.org/10.1093/bioinformatics/btt310.
65. Chikhi R, Rizk G. Space-efficient and exact de Bruijn graph representation based on a Bloom filter. Algorithms for Molecular Biology. 2013;8(1):22+. Available from: http://dx.doi.org/10.1186/1748-7188-8-22.

66. Artemov GN, Peery AN, Jiang X, Tu Z, Stegniy VN, Sharakhova MV, et al. The Physical Genome Mapping of Anopheles albimanus Corrected Scaffold Misassemblies and Identified Interarm Rearrangements in Genus Anopheles. G3: Genes— Genomes— Genetics. 2017;7(1):155–164.
67. Sharakhov IV, Artemov GN, Sharakhova MV. Chromosome evolution in malaria mosquitoes inferred from physically mapped genome assemblies. Journal of Bioinformatics and Computational Biology. 2016 Apr;14(2):1630003. Available from: http://dx.doi.org/10.1142/S0219720016300033.
68. Clark AG, Messer PW. Conundrum of jumbled mosquito genomes. Science. 2015;6217(347):27–28. Available from: http://dx.doi.org/10.1126/science.aaa3600.
69. Pombi M, Caputo B, Simard F, Di Deco MA, Coluzzi M, della Torre A, et al. Chromosomal plasticity and evolutionary potential in the malaria vector Anopheles gambiae sensu stricto: insights from three decades of rare paracentric inversions. BMC Evolutionary Biology. 2008 Nov;8:309.
70. Biller P, Guéguen L, Knibbe C, Tannier E. Breaking good: accounting for the diversity of fragile regions for estimating rearrangement distances. Genome Biology an Evolution. 2016;8:1427–1439.
71. Lin Y, Nurk S, Pevzner PA. What is the difference between the breakpoint graph and the de Bruijn graph? BMC Genomics. 2014;15 Suppl 6:S6.
72. Denton JF, Lugo-Martinez J, Tucker AE, Schrider DR, Warren WC, Hahn MW. Extensive Error in the Number of Genes Inferred from Draft Genome Assemblies. PLoS Computational Biology. 2014 Dec;10(12):e1003998+. Available from: http://dx.doi.org/10.1371/journal.pcbi.1003998.
73. Williams LJS, Tabbaa DG, Li N, Berlin AM, Shea TP, MacCallum I, et al. Paired-end sequencing of Fosmid libraries by Illumina. Genome Research. 2012;22(11):2241–2249.
74. Edgar RC. MUSCLE: Multiple sequence alignment with high accuracy and high throughput. Nucleic Acids Research. 2004;32(5):1792–1797.
75. Talavera G, Castresana J. Improvement of phylogenies after removing divergent and ambiguously aligned blocks from protein sequence alignments. Systematic Biology. 2007;56(4):564–77. Available from: http://www.ncbi.nlm.nih.gov/pubmed/17654362.
76. Stamatakis A. RAxML-VI-HPC: Maximum likelihood-based phylogenetic analyses with thousands of taxa and mixed models. Bioinformatics. 2006;22(21):2688–2690.
77. Sahlin K, Street N, Lundeberg J, Arvestad L. Improved gap size estimation for scaffolding algorithms. Bioinformatics. 2012;28(17):2215–2222.
78. Altschul SF, Gish W, Miller W, Myers EW, Lipman DJ. Basic local alignment search tool. Journal of Molecular Biology. 1990 Oct;215:403–410.
79. Goodman M, Czelusniak J, Moore GW, Romero-Herrera AE, Matsuda G. Fiiting the gene lineage into its species lineage, a parsimony strategy illustrated dy cladograms constructed from globin sequences. Systematic Zoology. 1979;28(2):132–163. Available from: http://scholar.google.com/scholar?hl=en{&}btnG=Search{&}q=intitle:No+Title{#}0.

Supplementary text

The ADSEQ algorithm: Gibbs-Boltzmann probabilistic framework

The sampling mode of ADSEQ is based on the following principle. For a given ADSEQ instance, let $\mathcal{A}$ be the set of all possible evolutionary scenarios that are in the search space considered by the dynamic programming algorithm. For a given scenario $A \in \mathcal{A}$, we denote by $s(A)$ its parsimony score. For a given *pseudo-temperature* kT, we define the *partition function* $Z_\mathcal{A}$ as follows:

$$Z_\mathcal{A} = \sum_{A\ in\mathcal{A}} e^{-s(A)/kT}$$

The Gibbs-Boltzmann probability of A is then

$$P(A) = \frac{e^{-s(A)/kT}}{Z_\mathcal{A}}$$

ADSEQ can sample solutions from $\mathcal{A}$ with each solution A having probability $P(A)$ to be sampled. In order to sample more frequently parsimonious or near-parsimonious scenarios, one can then tune the value of kT. While kT decreases toward 0, the probability mass of the parsimonious scenarios in the Gibbs-Boltzmann distribution increases, tending toward a uniform distribution over all parsimonious scenarios; conversely, when kT increases, the Gibbs-Boltzmann distribution evolves toward the uniform distribution over all scenarios. For extant adjacencies prediction, a *scaffolding propagation index (SPI)* parameter, allowing to propagate an extant adjacency of a species A in species B located in the same clade that species A with clade size equivalent to the value of *SPI* parameter, have been fixed to 20 (> 18) to consider synteny signal from every species during scaffolding procedure. For more information on ADSEQ algorithm, see [53].

Genome assemblies and sequencing data of 18 *Anopheles* genomes data set

Out the 18 *Anopheles* species, 16 have been sequenced genomes in [4] (see Tab. 2 for Genome assembly name). Paired sequencing data are available and were obtained from the Sequence Read Archive (SRA) of the NCBI with SRA-toolkit (see Tab. 2 for information on sequencing data). The whole set of 16 species with sequencing data have two sequencing libraries on a single female mosquito. A Paired-End library with an insert size of 180bp (called 'fragment' library) with FR orientation (→←) and a Mate-Pair library with an insert size of 1.5kbp (called 'jump' library) with RF orientation (←→). For 11 of them, a third insert size library of ∼38kbp (called 'fosill' library) was generated from a pool of hundred mosquitoes to improve the scaffolding with a FR orientation (→←). 'fosill' library is a Paired-End sequencing of fosmid library on Illumina that uses bacterial plasmid to integrate large genome portion to produce large insert size library (see [73] for more information). ID of Gene sets used for genome annotation of the 18 *Anopheles* are given in the Tab. 2. These gene sets were built by VectorBase in collaboration with J. Craig Venter Institute and/or the Broad Institute.

Pipeline to produce input data of ADSEQ for the 18 *Anopheles* genomes data set

We developed a pipeline to process available genomic data in input data for ADSEQ. Our pipeline is divided in two parts, first part consists to process genome content data and second part consists to process sequencing data. The pipeline is illustrated in Fig. 6.

Genome content data processing.

The right part (blue) of the pipeline in Fig. 6 consists to take available genome content and phylogenetic data on 18 *Anopheles* dataset to determine the list of adjacencies between gene contained in gene trees.

Initial filtering of gene families. First step consists to discard gene families for which, in at least one species, one gene is fully included within another gene, as such situation do not allow to unambiguously decide the relative position of the two genes (steps 1 and 2 of Fig. 6). This filter results in 14,981 gene families whose the content is illustrated in the middle graph of Fig. 8. For overlapping genes, there is no discarding of their gene families and adjacencies between these genes is determined by the relative position of their 5' position on the forward strand.

Computing reconciled gene trees. To handle the issues of erroneous gene trees in the gene trees dataset produced by Neafsey *et al.* [4], we inferred new gene trees from the 14,981 gene families with the protocol described in Fig. 7). For each gene family, CDS for the genes member of the family, obtained from VectorBase, were aligned with MUSCLE [74] (v3.8.425), then GBLOCKS [75] (v0.91b) was used to select high confidence alignment sites (columns). 41 families in which some sequences were not represented in any selected site were discarded at this step (see right graph of Fig. 8 for gene and species content of the 14 940 families). Maximum likelihood gene trees were then obtained with RAXML [76] (v8.2.8) with the GTR-GAMMA model, and 100 bootstrap iterations.

The maximum likelihood gene trees so obtained were then processed with PROFILENJ [59] to correct the topology by possibly changing branches with bootstrap support lower than 100% by minimizing the number of duplications and losses in a reconciliation with the considered specie tree.

In the less than one hundred cases where PROFILENJ generated several optimal solutions, an arbitrary topology was chosen. The result is a set of 14,940 gene trees representing 183,680 genes.

The resulting unrooted gene trees were then rooted and reconciled with the species tree using ECCETERA [54]. ECCETERA is a gene tree / species tree parsimony reconciliation algorithm that associates to every ancestral gene of a gene tree a species and an evolutionary event (speciation or duplication), choosing an assignment that minimizes the number of gene duplication and gene loss induced by the assignment. Given an unrooted gene tree, ECCETERA computes the rooting of the gene tree, among all possible ones, that minimizes the reconciliation score as defined above. The algorithm of ECCETERA is an efficient dynamic programming algorithm that process an unrooted gene tree with n leaves and a given species tree with m leaves in time $O(n^2m)$.

Observed gene adjacencies were deduced from annotated genes after removing of those that were not present in gene families, as ADSEQ relies on gene trees to infer ancestral and extant adjacencies (step 4 of Fig. 6). For statistics on the number of contigs and gene before and after the pipeline of data preprocessing, see Tab. 4.

Sequencing data processing.

The left part (green) of the pipeline in Fig. 6 consists to process paired-sequencing data to obtain weighted potential adjacencies. These adjacencies will be taken in account by DECOSTAR for more accurate prediction of new extant adjacencies and reconstruction of the evolutionary history of genome structure.

First step consisted to trimmed reads with TRIMMOMATIC (v0.36) [60] (step A of Fig. 6). Then trimmed reads have been mapped with BOWTIE2 (v2.2.9) [61] (step B of Fig. 6). Mapping were done on the three different insert size libraries with option allowing to take into account all alignments for each reads (see Tab. 2 for library insert size estimation from mapping). Except for *Anopheles arabiensis* & *Anopheles merus* where the 100 best alignments have been taken into account, due to excessive time computation (more than one month).

A scaffolding step is done to compute a score between contigs pairs linked with the scaffolding tool BESST (v2.2.6) [62,63] (Step C of Fig. 6). The following parameters have been used for BESST: –print_scores -z 10000 –min_mapq 0. BESST computes the gap distance between contigs pairs linked by paired-reads for which ones the distance is inferior to ($\mu + 3\sigma$), where μ and σ are respectively the mean and the standard deviation of the insert size library and determined by maximum likelihood estimation with GAPEST [77]. Then the method compute two scores, the link variation score (π_σ) and the link dispersity score (π_ζ)) for large contigs pairs (with size superior to ($\mu + 4\sigma$)). π_σ measures of how far observed distances are from the theoretical distance (where a π_σ =1 indicates that observed distances between contigs given by paired reads are similar to the estimated gap distance by GAPEST) and the π_ζ measures the similarity of reads distribution on contigs linked (where a π_ζ =1 indicates an exact similarity between the reads distribution observed on the two contigs). The number of scaffolding adjacencies and the scores distribution of these adjacencies are described in Fig. 10 and 11.

Finally, scaffolding adjacencies of annotated genome contigs pairs with more than 3 links (paired-reads) have been kept, because π_ζ score computed by BESST works correctly for scaffolding edges supported by more than 3 links, representing 405,939 directed contigs pairs linked by 4,128,682 scaffolding edges. If we consider only contigs containing genes present in gene trees *i.e* scaffolding gene adjacencies, total count for the whole *Anopheles* dataset is 68,876 scaffolding adjacencies use as input of ADSEQ and linked by 846,045 paired-reads .

Analysis of the newly inferred gene trees.

To evaluate the properties of the gene trees we inferred, we ran ADSEQ on two sets of gene trees: the gene trees obtained from *Anopheles* consortium (called RAW trees from now) and the gene trees we inferred (called PROFILENJ trees). The results are strikingly different. For example the RAW gene trees yield 39,194 duplications, against 6,461 for PROFILENJ gene trees. Fig. 5 summarizes two ancestral genomes statistics of interest. On the left-hand side we represent the distribution of the number of genes in ancestral genomes. Some ancestral genomes can have more than 30,000 genes in the RAW dataset, three times more than the biggest extant genome. Numbers are much more reasonable with the ProfileNJ dataset. On the right-hand side, we illustrate the linearity of ancestral genomes. recall that genomes do not have to be strictly linear as an output of ADseq (before linearization). We use the distribution of degrees of ancestral genes, defined as follows: the degree of a gene is the sum of the ADseq *posterior* score (that belongs to $[0, 1]$) of all adjacencies involving this gene. We use this statistics as a measure of the linearity of the inferred genomes. The ideal gene degree distribution of a complete error-free genome assembly is illustrated in the black graph (almost all genes have exactly two adjacencies and so degree two). It appears clearly that the ProfileNJ distribution (red graph) is much closer to the ideal than the RAW distribution (blue graph).

All metrics argue in favor of ProfileNJ trees for better ancestral genome inference. However, the results show gaps between the ideal scenario and ProfileNJ values. This may be due to a reconciliation with duplications and losses, while a lot of genes introgress, phylogenetic artifacts (some wrong branches are highly supported by bootstrap), errors in multiple sequences alignments or in clustering genes into families, or false positives in ADseq ancestral adjacencies.

The ADseq validation protocol

After species selection and random sampling of sequencing data (steps 1 and 2 of Fig. 12), reads are mapped with the method Minia (v2.0.3) with default parameter (except parameter abundance-min fixed to 3) (step 3 of Fig. 12). KmerGenie (v1.7016) has been used with default parameter to determine the best kmer size value use as input of Minia (see Tab. 2 for kmer size used). In order to be able to compare the new assembly with the initial assembly, we aligned the new contigs onto the initial assembly using BLASTn (v2.4.0+) [78] with BLASTn algorithm (with -task megablast) and e-value threshold fixed to 1E-10. To transfer gene annotation from initial to the new assembly, Minia contigs have to be uniquely and confidently mapped on contigs of reference assembly (step 4 of Fig. 12). To insure these criterion, two filters have been applied. Filter 1 consists to keep only contig alignment with $identity >= 90\%$ and $coverage >= 90\%$. On the remaining contig alignments only contigs with an unique optimal score alignment (in identity and coverage) are kept (Filter 2). Moreover, if alignments of two contigs overlap the same gene, we join them into a single contig, simulating a scaffolding step based on transcripts (Merging step). Finally, any gene family for which at least one gene does not align with the new contigs is completely discarded from the initial data and from the remaining analysis (Filter 3). See Tab. 3 for assembly statistics at the different filtering step of the Minia contigs gene annotation. Then, Minia contigs are scaffolded to get adjacencies with sequencing support (step 5 of Fig. 12). The pipeline is the same that those used for the analysis of the 18 *Anopheles* dataset (see Fig. 6 and SI text) at the exception of the number of read multiple alignments in Bowtie2 limited to 50 to reduce the computation time. After scaffolding step, all input data necessary for DeCoSTAR are ready. We apply DeCoSTAR on input data with (ADseq) or without (AD) sequencing data to predict new adjacencies (step 6 of Fig. 6).

Then, last part of the pipeline consists to compute precision and recall statistics on predicted adjacencies compare to adjacencies not present in Minia contigs but in reference contigs.

Comparison of scaffolding accuracy of ADseq, AD and BESST on simulated fragmented genomes

After genome fragmentation simulation for the three selected species (*Anopheles albimanus*, *Anopheles arabiensis* and *Anopheles dirus*) and the two reads sampling (50% and 100%). ADseq, AD and BESST are applied on the 6 datasets (3 species x 2 reads sampling) to compare the ability of the three methods to scaffolds genome. For each condition, first step consists to determine list of adjacencies that have been occulted during genome fragmentation simulation. Set of predicted of the three scaffolding methods are compared to this list. For BESST, set of predicted adjacencies corresponds to adjacencies as output of BESST and is not limited to adjacencies for which BESST compute scores. For AD and ADseq, set of predicted adjacencies corresponds to predicted adjacencies after linearization of genome on adjacencies with *a posteriori* support upper or equal to 0.1, 0.5 or 0.8 (see Methods). These values have been chosen after drawing the precision and recall statistics distribution in function of the support threshold filter used for predicted adjacencies. These distributions are plotted in Fig. 14 (where gene orientation is considered to determine an adjacency as TP) and Fig. 15 (where gene orientation is not considered to annotate an adjacency as TP). These distributions show that there are switch for a threshold value set to 0.5. Under 0.5, ADseq and AD have a lower precision but stronger recall and for a threshold upper 0.5 a stronger precision and lower recall.

Supplementary figures

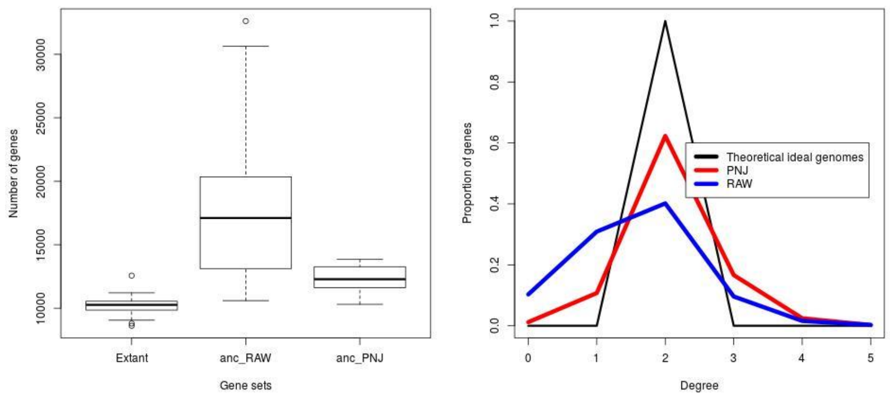

Figure 5 Extant and ancestral genome gene content (left) and ancestral gene degree (right). Left: Number of genes of extant species (left), ancestral species using the reconciled VectorBase gene trees (middle), and ancestral species using the reconciled ProfileNJ gene trees (right). Right: Gene degree distribution of ancestral genes after applying ADseq with the RAW gene trees (blue graph) and the ProfileNJ gene trees (red graph), compared to the expected gene degree distribution for theoretical perfectly assembled genomes (black graph). The degree of a gene is defined as the sum of the ADseq *posterior* scores of adjacencies involving this gene. Here the value at coordinate x is the sums of all degrees in the interval $[x, x+1[$

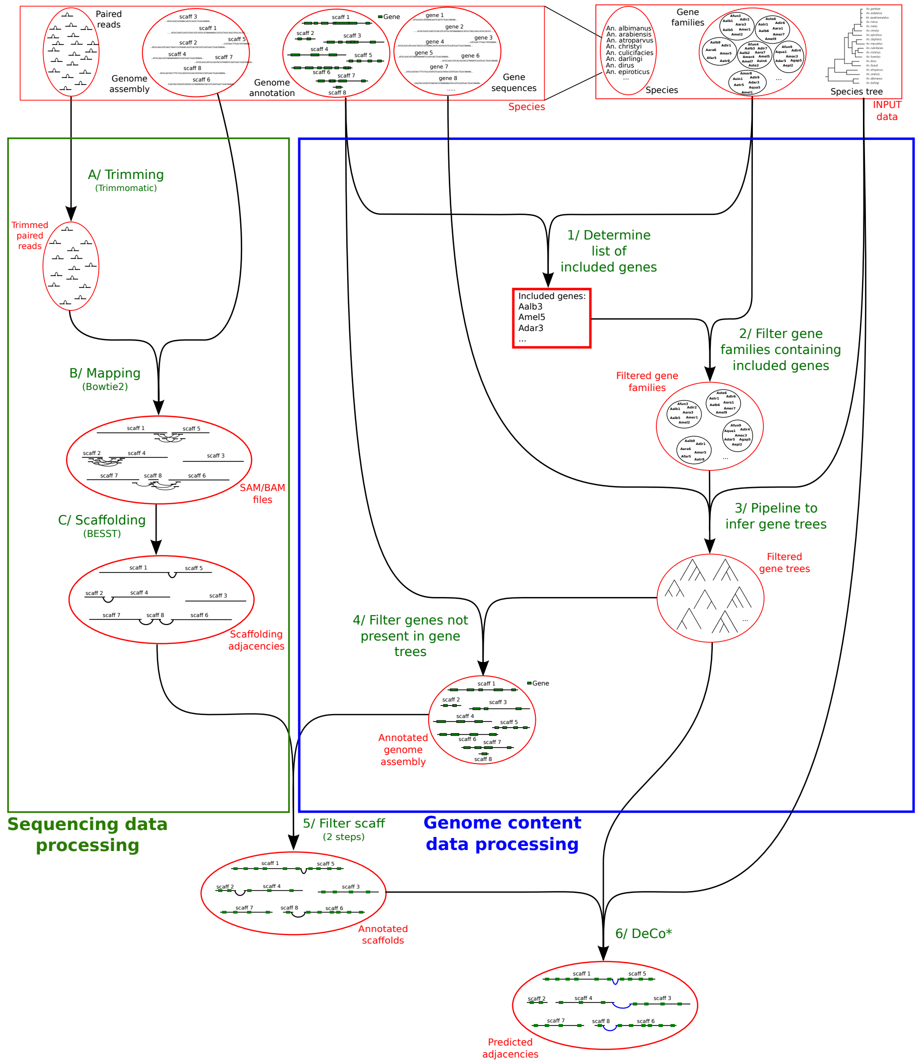

Figure 6 Pipeline to produce input data for ADseq on 18 Anopheles dataset. The pipeline takes as input a species tree for the 18 *Anopheles* species, the whole set of gene families and gene trees for these species and genomic data (contigs, scaffolds and chromosomes). The goal of the pipeline is to produce input data for the ADSEQ algorithm to reconstruct ancestral genome structure and evolution and to improve extant genome scaffolding. The pipeline is split into two parts: The first part (Blue one) processes genome content data to obtain extant genome adjacencies. **Step 1** detects genes that are included in other genes. In **step 2**, gene families containing these genes are filtered out to avoid ambiguity in defining observed extant gene adjacencies. In **step 3**, gene trees are inferred from the gene sequences, one gene tree per gene family (see Fig. 7 for more information on gene trees inference pipeline). Finally, in **step 4** genes contained in gene families for which gene trees have not been inferred are discarded from the analysis (41 gene families containing representing 1,039 genes). The second part of the pipeline (Green one) processes sequencing data to obtain scaffolding adjacencies that will be used to improve extant genome assembly with the ADSEQ algorithm. **Step A** trims reads with TRIMMOMATIC to remove low qualities reads and remaining adapters. In **Step B**, trimmed reads are mapped onto their respective genome with BOWTIE2 considering all multiple mappings. In **Step C**, pairs of contigs for which paired-end reads suggest a possible contiguity along their chromosome are linked with the scaffolding software BESST, and the resulting potential scaffolding adjacencies are scored according to the BESST model. Then, in **Step 5** scaffolding gene adjacencies are determined from contigs adjacencies obtained from sequencing data processing part with genes present in gene trees. This results in scaffolds with observed scored scaffolding adjacencies that are used as input of DECOSTAR (**step 6**). See Tab. 4 for a description per species on dataset used for DECOSTAR.

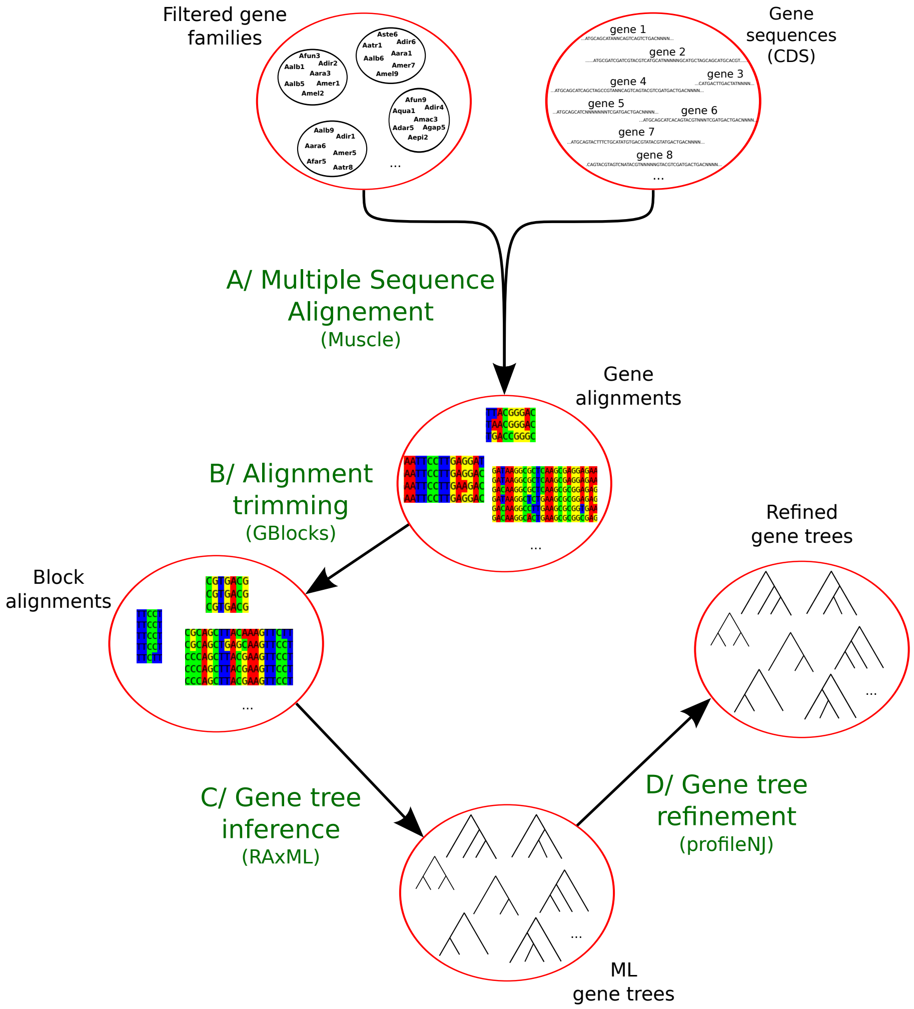

Figure 7 Pipeline to improve gene trees inference from homologous gene family. CDS sequences of genes in gene trees have been obtained from VectorBase database and homologous gene families deduced from the 14,981 gene trees resulting of step 2 of Fig. 6. **Step A** consists to multiple align homologous genes with MUSCLE with parameter "-maxiters 2" if a gene sequence have a size upper than 32,000 bp. In **step B**, GBLOCKS was applied on alignments to select high confidence alignment sites. At this step, 41 gene families have been discarded due to sequences that were not present in a selected blocks. For **step C**, RAxML have been used to infer maximum likelihood gene trees with the GTR-GAMMA model and 100 bootstrap iterations. Finally in **step D**, the maximum likelihood gene trees are processed with PROFILENJ to potentially changing branches with bootstrap support lower than 100% in a DL reconciliation model (min(Duplication,Loss)) with the species tree [79].

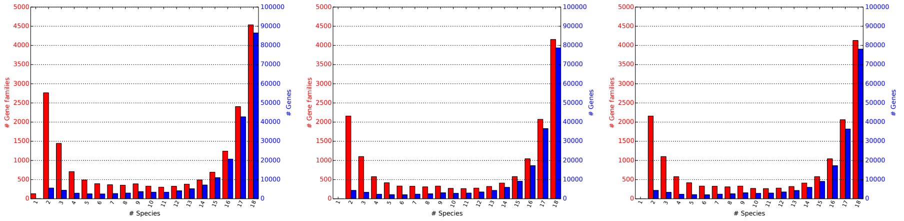

Figure 8 Distribution, per species, of gene families number (red bars) and number of genes (blue bars). Left graph: distribution of the 17,780 raw input gene trees corresponding to 212,800 genes. **Middle graph:** distribution of the 14,981 gene families, containing 184,719 genes, after discarding families containing included genes (after step 2 of Fig. 6). **Right graph:** distribution of the 14,940 gene trees, composed of 183,680 genes, after gene trees inference pipeline (after steps 3 and 4 of Fig. 6).

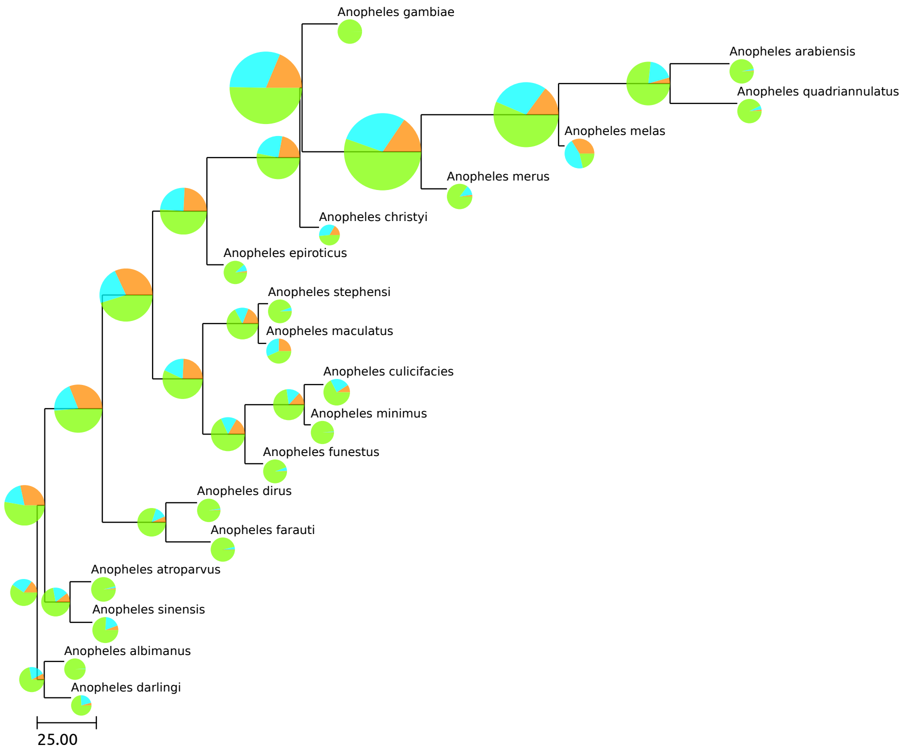

Figure 9 Anopheles species trees (X phylogeny) with rearrangements per adjacency as branch lengths ($.10^{-3}$), obtained using the RAW gene trees. The pie chart for a given species represents the adjacency degree of the genes of this species: orange represents genes with no adjacency, light blue gene with adjacency degree of 1 and green genes with adjacency degree of 2. Moreover, the diameter of each chart is proportional to the number of genes in the corresponding species.

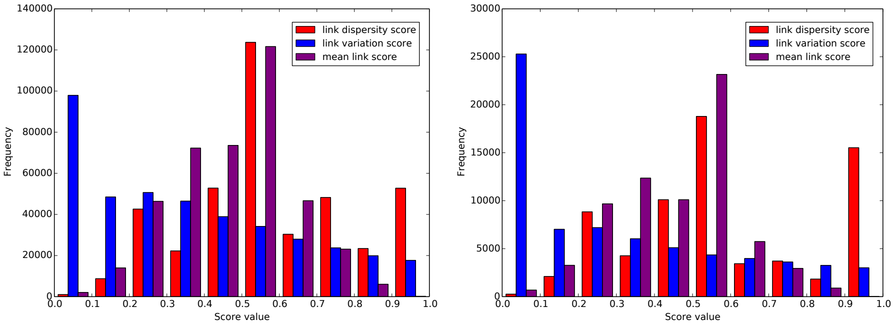

Figure 10 Distributions of scaffolding adjacencies scores computed by BESST for scaffolding adjacencies supported by at least 3 paired reads. Left graph: adjacency scores distribution between all contigs or scaffolds, over 405,939 scaffolding adjacencies. **Right graph:** adjacency scores distribution for contigs and scaffolds with gene corresponding to the 68,876 scaffolding gene adjacencies considered by DeCoSTAR. Blue bars represent the link variation score, red bars the link dispersity score and purple bars the mean of the two link scores. For more information on the link scores see SI text and [70].

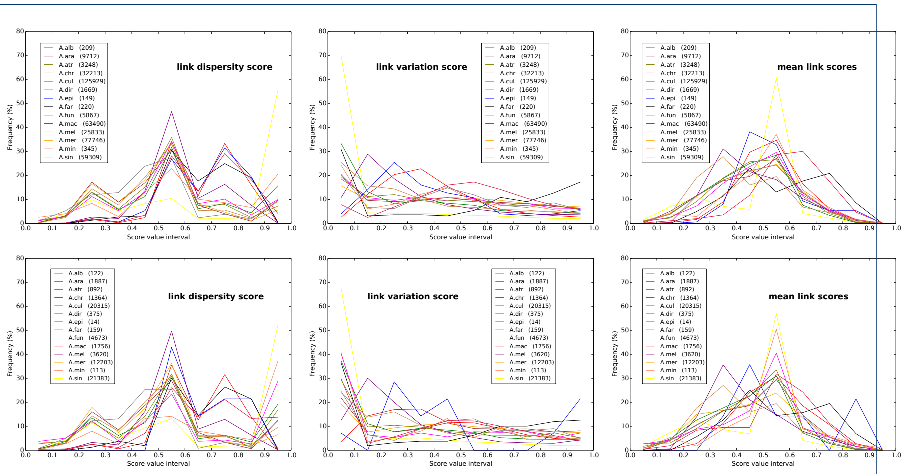

cmcm

Figure 11 Distributions of scaffolding adjacencies link scores computed by BESST for scaffolding adjacencies supported by at least 3 paired reads, for each of the 18 Anopheles species. Upper graphs: distribution of scores all 405,939 potential scaffolding adjacencies. **Lower graphs:** distribution of scores for all 68,876 scaffolding gene adjacencies used as input by DeCoSTAR. **Left graphs:** distribution of link dispersity scores. **Middle graphs:** distribution of link variation scores. **Right graphs:** distribution of the mean of link variation and dispersity scores. Each color corresponds to one species and the number between parenthesis in the legend indicates the number of scaffolding adjacencies inferred by BESST for each species.

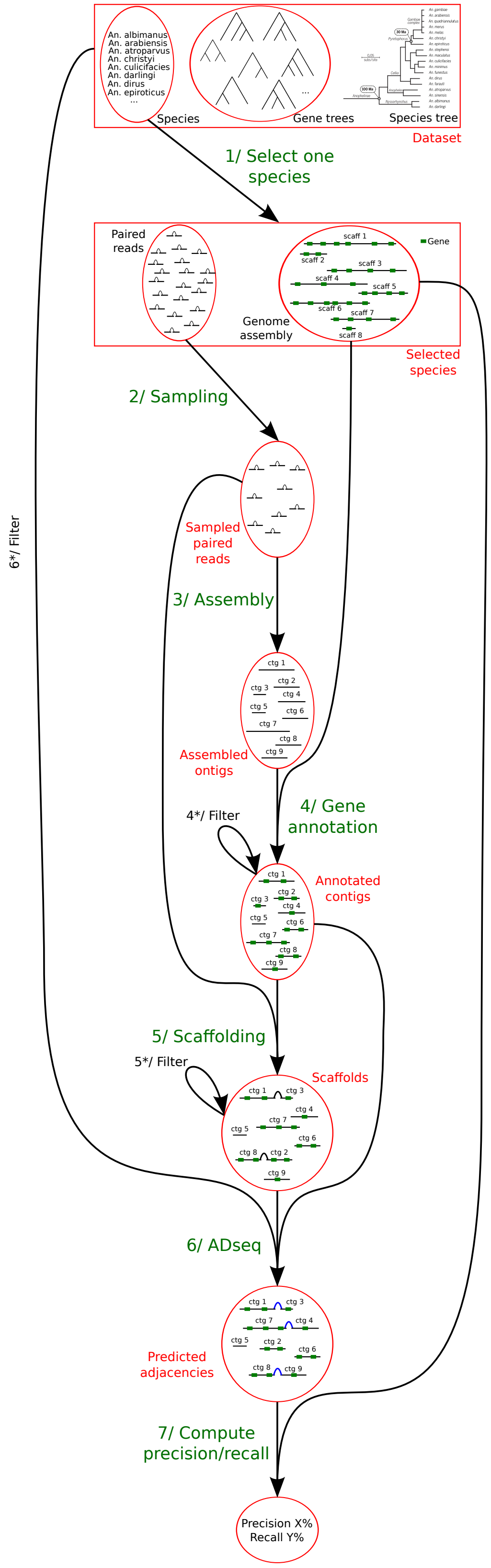

Figure 12 The ADseq validation protocol

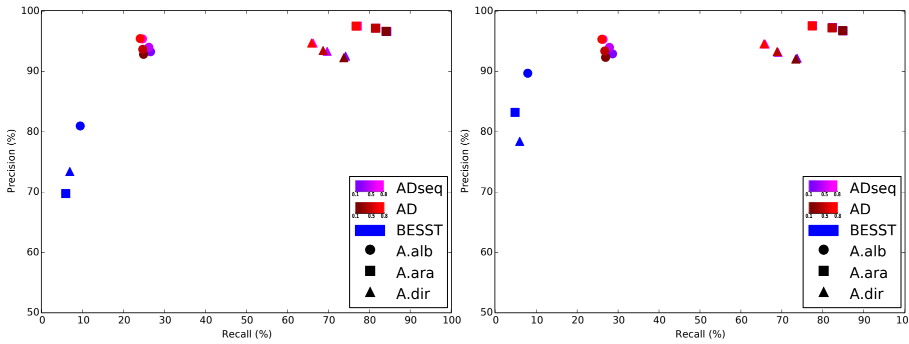

Figure 13 Precision and recall statistics for scaffolding adjacencies on three artificially fragmented genomes (A.alb: Anopheles albimanus, A.ara: Anopheles arabiensis and A.dir: Anopheles dirus), when gene orientations are not accounted for. Left graph: results with 50% of reads. **Right graph:** results with all reads. The different methods results are plotted with the precision on the Y axis and the recall on the X axis. For ADSEQ and AD, results for three different adjacency support threshold (0.1, 0.5 and 0.8) before genome linearization are plotted and represented with a color gradient. These results show similar results to Fig. 2 showing that for most of the predicted adjacencies the three methods infer the correct gene orientation.

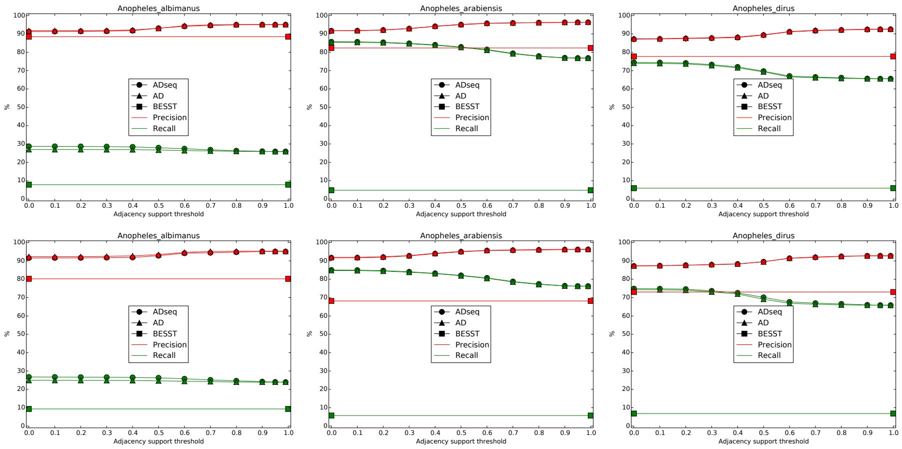

Figure 14 Distributions of precision and recall statistics for new extant adjacencies prediction on three artificially fragmented genomes compared to reference genome assemblies. Upper graphs: statistics with a sample of 50% of the reads. **Lower graphs:** statistics with all reads. Each graph corresponds to one of the three species for which genome has been fragmented by simulation (*An. albimanus*, *An. arabiensis* and *An. dirus*). precision and recall statistics are plotted in function of the threshold applied on the support of predicted adjacencies in ADSEQ and AD. Genomes are not linearized in this analysis. Note: To determine a gene adjacency as True Positive (TP), the gene involved in the adjacency have to be inferred in the proper orientation.

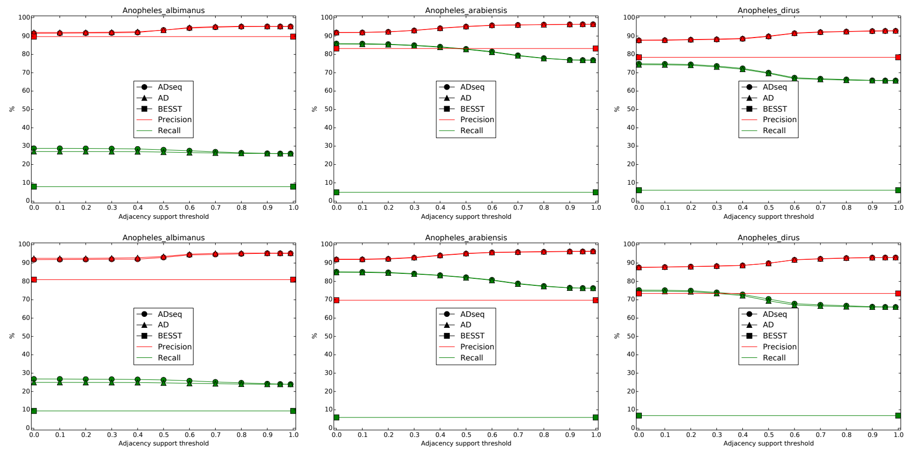

Figure 15 Similar to Fig. 14 but without accounting for gene orientation.

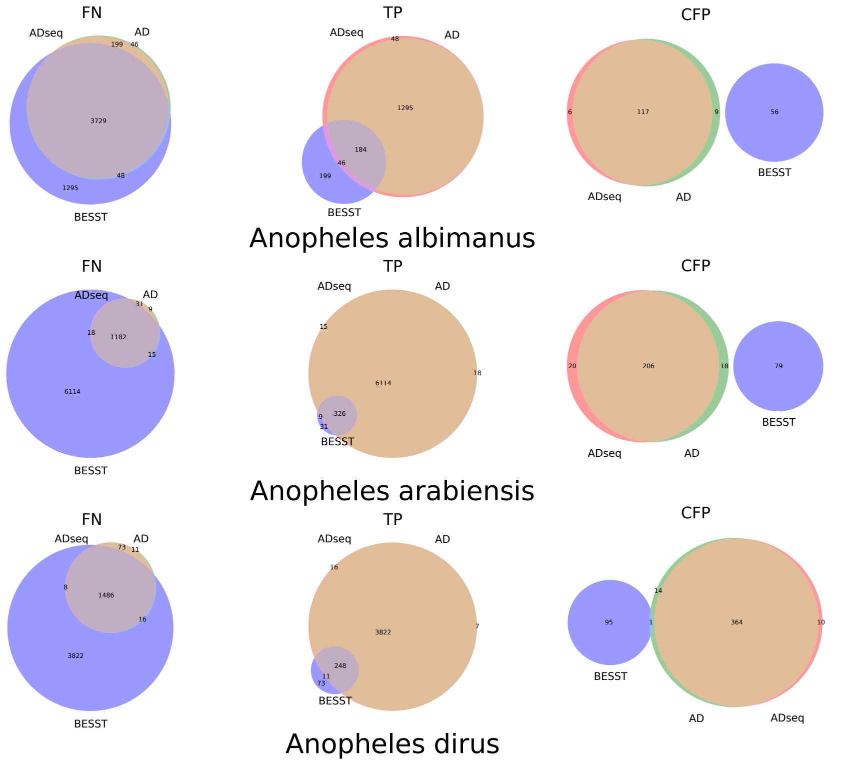

Figure 16 Venn diagrams showing adjacencies shared by the three scaffolding methods ADseq, AD and BESST with a sample of 50% of the reads. **Upper Venn diagrams:** results for *Anopheles albimanus*. **Middle Venn diagrams:** results for *Anopheles arabiensis*. **Lower Venn diagrams:** results for *Anopheles dirus*. **Left diagrams:** False Negative (FN) adjacencies, corresponding to adjacencies created by the fragmentation process and that have not been recovered. **Center diagrams:** results for True Positive (TP) adjacencies. Here, an adjacency is considered TP if the pair of genes is adjacent in the reference assembly and the orientation of genes involved in the adjacency is properly recovered. **Right diagrams:** results for Certain False Positive (CFP) adjacencies. An adjacency is determined as CFP when the pair of gene does not belong to the reference assemblies and one of the two genes is not located at a contig extremity in reference genome, or if the recovered orientation of genes is incorrect. If we consider method individually, these results show that ADSEQ outperforms AD and BESST with the lowest number of FN adjacencies, the largest number of TP adjacencies and the lowest number of CFP adjacencies (except for *An. albimanus* where AD has the lowest number of CFP (224 vs. 226 for ADSEQ). However, if we combine *a posteriori* AD and BESST, this performs better ADSEQ in terms of recall (higher number of TP adjacencies) but at the expense of a strong decreases of precision (much higher number of CFP adjacencies).

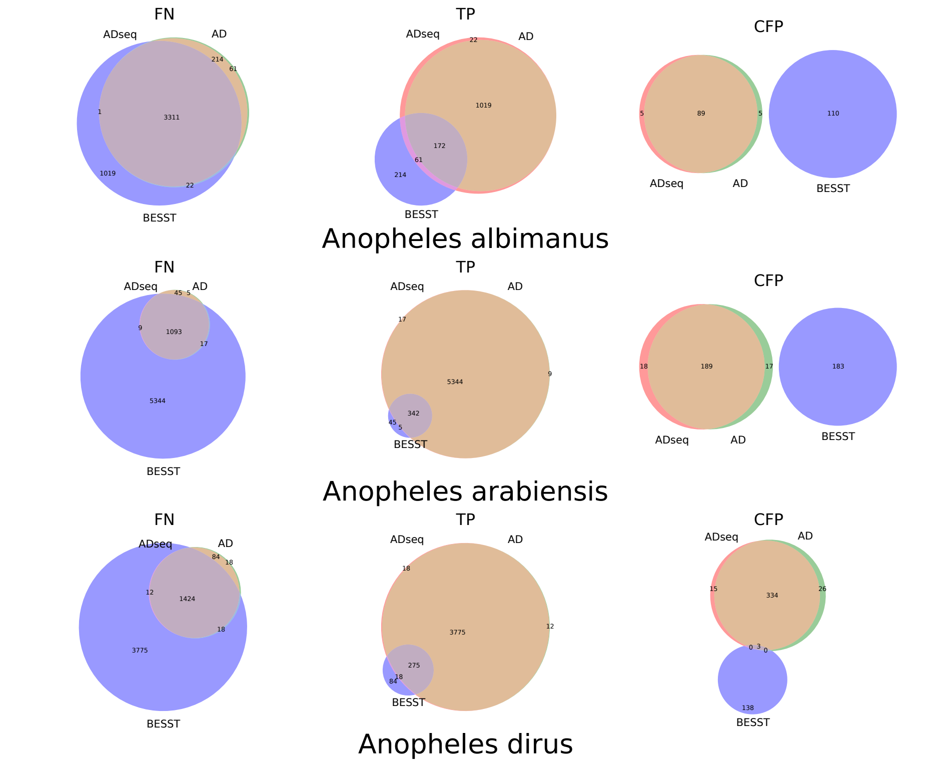

Figure 17 Similar to Fig. 16 with all reads included.

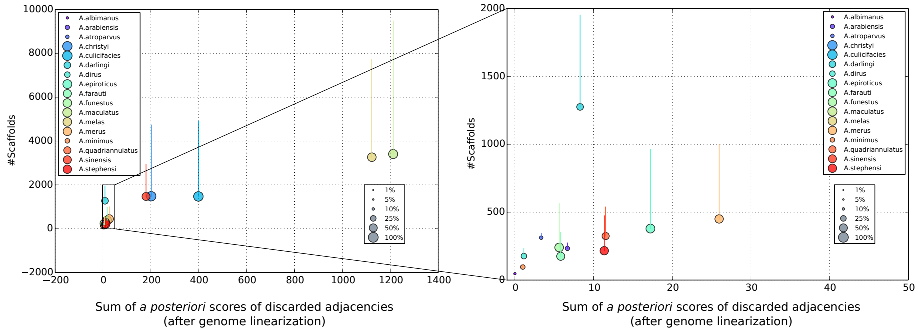

Figure 18 Scatter plot exhibiting scaffolding improvement of the 18 Anopheles genomes by ADseq with X species tree phylogeny. Right plot is a zoom of a small part of the left graph. Each color corresponds to one species. For each species, upper part of vertical line corresponds to number of segments in initial assembly and lower part the number of segments after scaffolding improvement by ADSEQ. Circle diameter is proportional to the % of scaffolding improvement of the genome where scale is displayed in lower right part of the graphs.

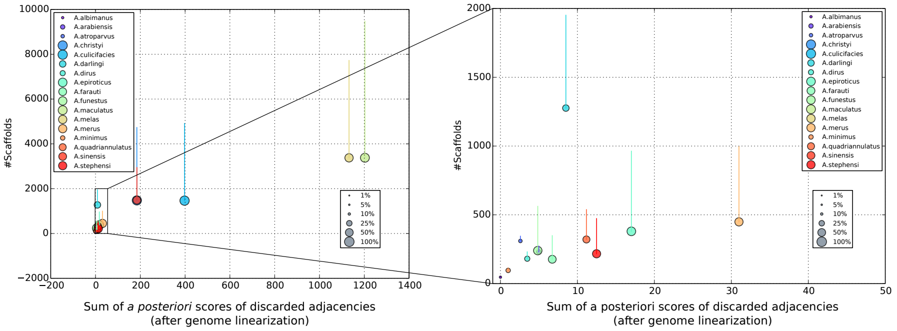

Figure 19 Similar to Fig. 18 with WG species tree phylogeny.

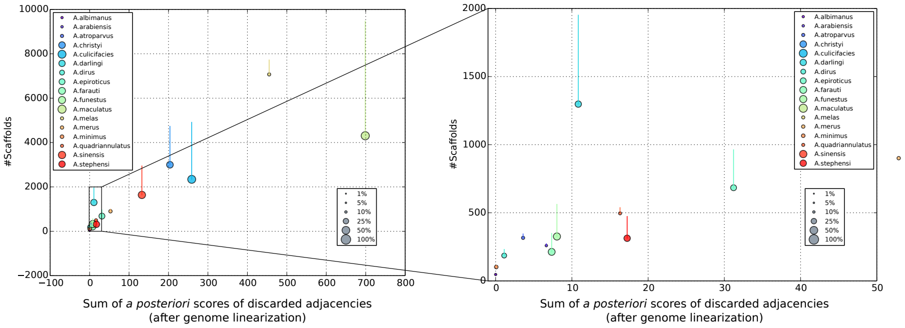

Figure 20 Similar to Fig. 18 with RAW gene trees instead of ProfileNJ gene trees.

Supplementary tables

Species name	Assembly name	Gene set	BioProject	Library name	SRA ID	Median insert size (bp)
An. albimanus	AalbS1	AalbS1.1	PRJNA67235	’fosill’	SRX200219	35,557
				’jump’	SRX111456	2,408
				’fragment’	SRX084279	194
An. arabiensis	AaraD1	AaraD1.1	PRJNA67207	’fosill’	SRX200218	36,444
				’jump’	SRX111457	2,051
				’fragment’	SRX084275	195
An. atroparvus	AatrE1	AatrE1.1	PRJNA67233	’fosill’	SRX209222	36,897
				’jump’	SRX209384	2,408
					SRX209606	2,382
				’fragment’	SRX209390	191
					SRX209612	191
An. christyi	AchrA1	AchrA1.1	PRJNA67213	’jump’	SRX110286	1,242
					SRX119723	1,229
				’fragment’	SRX084278	195
An. culicifacies	AculA1	AculA1.1	PRJNA163119	’jump’	SRX175835	546
					SRX334058	1,156
				’fragment’	SRX158118	181
					SRX182921	182
					SRX189771	183
					SRX272317	196
An. darlingi	AdarC2	AdarC2.2	NA	NA	NA	NA
An. dirus	AdirW1	AdirW1.1	PRJNA196855	’fosill’	SRX209221	36,451
				’jump’	SRX209379	2,378
					SRX209603	2,354
				’fragment’	SRX209381	191
					SRX209604	191
An. epiroticus	AepiE1	AepiE1.1	PRJNA191562	’jump’	SRX209380	854
					SRX209614	822
				’fragment’	SRX209391	191
					SRX209605	191
An. farauti	AfarF1	AfarF1.1	PRJNA67229	’fosill’	SRX349764	404
			PRJNA214011	’fosill’	SRX357088	405
					SRX357089	405
				’jump’	SRX111458	1,976
				’fragment’	SRX084280	175
An. funestus	AfunF1	AfunF1.1	PRJNA67223	’fosill’’	SRX209224	36,450
				’jump’	SRX209389	2,010
					SRX209610	1,979
				’fragment’	SRX209387	192
					SRX209628	192
An. gambiae	AgamP3	AgamP3.8	NA	NA	NA	NA
An. maculatus	AmacM1	AmacM1.1	PRJNA67215	’jump’	SRX209385	709
					SRX209609	682
				’fragment’	SRX209386	191
					SRX209629	191
An. melas	AmelC1	AmelC1.1	PRJNA163117	’jump’	SRX175836	651
				’fragment’	SRX158119	176
					SRX184877	177
					SRX189770	179
An. merus	AmerM1	AmerM1.1	PRJNA67215	’fosill’	SRX349762	37,890
					SRX357090	37,880
					SRX357091	37,882
				’jump’	SRX110236	1,383
				’fragment’	SRX084276	195
An. minimus	AminM1	AminM1.1	PRJNA67225	’fosill’	SRX209223	36,838
				’jump’	SRX209388	2,296
					SRX209608	2,272
				’fragment’	SRX209383	192
					SRX209627	192
An. quadriannulatus	AquaS1	AquaS1.1	PRJNA67209	’fosill’	SRX200216	37,429
				’jump’	SRX111455	2,137
				’fragment’	SRX084277	175
An. sinensis	AsinS1	AsinS1.1	PRJNA214011	’fosill’	SRX349763	38,486
					SRX357092	37,880
					SRX357093	37,882
				’jump’	SRX334057	2,373
				’fragment’	SRX334056	187
An. stephensi	AsteS1	AsteS1.1	PRJNA67219	’fosill’	SRX200217	34,405
				’jump’	SRX209378	2,244
					SRX209611	2,278
				’fragment’	SRX209382	171
					SRX209607	171

Table 2 Summary of genome assemblies and sequencing data information.

Explanations for Table 2. 16 on the 18 *Anopheles* species have been sequenced in [4] and data are available on the SRA database of the NCBI (see column 4 and 6 for BioProject and SRA ID). FASTQ files of paired sequencing data have been obtained with SRA-TOOLKIT. After mapping of paired reads on reference genome assemblies (column 2), median insert size of libraries have been determined with package "CollectInsertSizeMetrics" of PICARD TOOLS (v1.61) (column 7). Column "Library name" give information on the sequencing strategies employed in [4]. Where 'fragment' library corresponds to a Paired-End library with an expected insert size of 180bp and FR orientation (→←). 'jump' library corresponds to a Mate-Pair library with an insert size of 1.5kbp and RF orientation (←→). And 'fosill' corresponds to a library generated from a pool of hundred mosquitoes to improve the scaffolding with an expected insert size around 38kbp and FR orientation (→←). Column 3 gives the ID of gene set used in this study.

Species name	Assembly stats	Initial assembly	Minia assembly **(50% reads)**				
			initial	after filter1	after filter2	after merging	after filter3
An. albimanus	kmer size	NA	75				
	#CTG	204	93,906	86,698	86,307	5,555	5,547
	Size (bp)	170,508,315	170,159,531	167,477,606	167,368,303	69,154,374	69,071,024
	#gene)	NA				9,030	9,018
	N50 (bp)	18,068,499	4,833	4,908	4,911	17,015	17,013
	N50 (#gene)	NA				2	2
	#gene trees	NA				14,940	14,915
An. arabiensis	kmer size	NA	59				
	#CTG	1,214	302,287	243,251	238,596	7,974	7,968
	Size (bp)	246,567,867	231,833,497	219,419,350	218,591,584	64,718,036	64,675,874
	#gene	NA				10,274	10,268
	N50 (bp)	5,604,218	2,193	2,384	2397	11,132	11,123
	N50 (#gene)	NA				1	1
	#gene trees	NA				14,940	14,918
An. dirus	kmer size	NA	63				
	#CTG	1,266	220,053	164,611	160,972	5,892	5,888
	Size (bp)	216,307,690	217,905,932	202,370,679	201,700,338	89,145,793	89,115,176
	#gene	NA				9,789	9,781
	N50 (bp)	18,068,499	7,281	8,455	8,521	25,298	25,230
	N50 (#gene)	NA				2	2
	#gene trees	NA				14,940	14,846

Species name	Assembly stats	Initial assembly	Minia assembly **(100% reads)**				
			initial	after filter1	after filter2	after merging	after filter3
An. albimanus	kmer size	NA	83				
	#CTG	204	71,361	64,512	64,179	4,852	4,845
	Size (bp)	170,508,315	169,477,186	166,370,462	166,259,421	77,887,807	77,807,527
	#gene	NA				9,012	9,000
	N50 (bp)	18,068,499	7,564	7,688	7,705	21,801	21,801
	N50 (#gene)	NA				2	2
	#gene trees	NA				14,940	14,898
An. arabiensis	kmer size	NA	72				
	#CTG	1,214	229,218	184,605	181,423	7,133	7,127
	Size (bp)	246,567,867	232,286,601	219,658,117	218,990,676	80,623,434	80,568,561
	#gene	NA				10,253	10,246
	N50 (bp)	5,604,218	4,322	4,838	4,864	17,147	17,147
	N50 (#gene)	NA				1	1
	#gene trees	NA				14,940	14,896
An. dirus	kmer size	NA	75				
	#CTG	1,266	210,188	155,771	153,031	5,836	5,829
	Size (bp)	216,307,690	220,937,663	202,341,639	201,719,647	91,254,277	91,196,154
	#gene	NA				9,759	9,748
	N50 (bp)	18,068,499	7,666	9,044	9,115	27,134	27,141
	N50 (#gene)	NA				2	2
	#gene trees	NA				14,940	14,816

Table 3 Assembly statistics at various stages of the gene annotation step of validation protocol of ADseq (step 4 of Fig. 12). For each species and annotation step, table gives different assembly statistics (column2): the number of contigs in the assembly, the size of the assembly in bp and in gene number, the N50 statistics of the assembly in bp and in gene number (if available) and gene trees number corresponding to gene present in the assembly (for the two last columns). Column 3 (Initial assembly) corresponds to the assembly statistics of reference genomes. Columns 4-8 of upper and lower table corresponds to Minia assembly statistics at different filtering step respectively with 50% reads sampling and without reads sampling. Column "initial" corresponds to assembly in output of Minia algorithm assembly. Minia contigs are then mapped on reference genome to annotate gene of reference assembly on Minia contigs. Assembly statistics after filter1 corresponds to Minia contigs that have been mapped on reference assembly with an identity and a coverage $>= 90\%$. Filter2 consists to keep only contig with an unique optimal alignment (to avoid uncertainty in gene annotation). Column 7 corresponds to Minia assembly statistics after merging of Minia contigs overlapping a same gene (simulating RNA-seq scaffolding). Then last column corresponds to statistics after filter3 that consists to discard gene families of genes that have not been mapped on Minia contigs.

species name	initial dataset						post data preprocessing			
	all contigs		contigs with gene				contigs with gene			
	#CTG	N50 (bp)	#CTG	N50		#gene	#CTG	N50		#gene
				bp	#gene			bp	#gene	
An. albimanus	204	18,068,499	57	18,068,499	1,212	11,911	49	18,068,499	916	9,056
An. arabiensis	1,214	5,604,218	340	5,830,121	348	13,162	273	5,830,121	321	10,298
An. atroparvus	1,371	9,206,694	476	9,206,694	655	13,776	345	9,206,694	512	10,400
An. christyi	30,369	9,057	5,173	17,016	3	10,738	4,731	17,384	2	8,792
An. culicifacies	16,162	22,320	5,715	32,742	4	14,335	4,912	34,064	3	11,213
An. darlingi	2,160	115,168	2,161	115,168	10	10,457	1,951	118,843	9	8,617
An. dirus	1,266	6,906,475	302	7,656,907	543	12,781	231	7,656,907	406	9,883
An. epiroticus	2,673	366,526	1,052	417,110	29	12,078	963	425,117	24	9,855
An. farauti	550	1,196,527	376	1,235,781	84	13,217	349	1,235,781	64	10,239
An. funestus	1,392	671,960	619	702,105	46	13,344	562	703,988	36	10,077
An. gambiae	7	49,364,325	6	49,364,325	2,867	12,810	6	49,364,325	2,339	10,324
An. maculatus	47,797	3,841	12,776	4,751	1	14,835	9,473	5,042	1	10,552
An. melas	20,281	18,041	8,855	21,239	2	16,149	7,723	21,730	2	12,567
An. merus	2,753	342,196	1,078	391,600	886	13,887	997	400,239	23	10,736
An. minimus	678	10,313,149	142	10,313 149	886	12,560	114	10,313,149	682	9,792
An. quad.	2,823	1,641,272	647	1,794,736	95	13,349	538	1,846,441	74	10,289
An. sinensis	11,270	80,738	3,536	103,937	9	14,791	2,944	109,624	7	10,962
An. stephensi	1,110	837,295	502	851,727	57	13,113	473	851,727	44	10,028
All species	144,080	760,870	43,813	1,159,817	45	237,293	36,634	1,272,063	37	183,680

Table 4 Assembly statistics on the 18 Anopheles genomes. Statistics before before processing are displayed in columns 2-7 and after the pipeline to produce input data for the DeCoSTAR algorithm in columns 8-11 (see Fig. 6 for illustration of the data preprocessing step). For initial dataset assembly statistics, columns 2 and 3 present contigs number and N50 statistic in bp for all contigs in genome assemblies. In columns 4-7, only contigs with at least one gene are considered. Column 4 corresponds to contigs number with gene in reference assemblies. Columns 5 & 6 represent N50 statistics respectively in bp and in gene number. Column 7 represent the number of gene in reference genome assemblies. For genome assemblies used as input of DeCoSTAR, all contigs contains at least one gene. Column 8 gives the number of contigs after step 4 of Fig. 6. Columns 9 & 10 represent N50 statistics respectively in bp and in gene number. And column 11 represents the number of gene in genomes taken as input of DeCoSTAR. The input dataset of DeCoSTAR is composed of 14,940 gene trees (see Figs. 8 and 7 for more information on gene trees) and 68,876 gene adjacencies with sequence support (scaffolding gene adjacencies) (see Figs. 10 and 11 for more information on scaffolding adjacencies).

Species name	Genome assemblies before ADseq				Genome scaffolds after ADseq **(X topology)**			
	contigs with gene				scaffolds with gene			
	#CTG	N50		#gene	#scaffolds	N50		#new adj (#scaff adj)
		bp	#gene			bp	#gene	
An. albimanus	49	18,068,499	916	9,056	47	18,068,499	916	2 (2)
An. arabiensis	273	5,830 121	321	10,298	216	9,217,108	410	57 (13)
An. atroparvus	345	9,206,694	512	10,400	306	10,083,987	647	39 (12)
An. christyi	4,731	17,384	2	8,792	1,396	95,212	12	3,335 (204)
An. culicifacies	4,912	34,064	3	11,213	1,339	202,550	19	3,574 (1,366)
An. darlingi	1,951	118,843	9	8,617	1,264	197,002	13	687 (NA)
An. dirus	231	7,656,907	406	9,883	176	17,377,229	778	55 (10)
An. epiroticus	963	425,117	24	9,855	369	1,611,558	78	594 (7)
An. farauti	349	1,235,781	64	10,239	169	2,391,621	146	180 (64)
An. funestus	562	703,988	36	10,077	231	2,772,343	127	331 (112)
An. gambiae	6	49,364,325	2,339	10,324	6	49,364,325	2,339	0 (NA)
An. maculatus	9,473	5,042	1	10,552	3,025	30,779	7	6,448 (295)
An. melas	7,723	21,730	2	12,567	2,685	92,676	9	5,038 (165)
An. merus	997	400,239	23	10,736	419	1,183,618	65	578 (391)
An. minimus	114	10,313,149	682	9,792	96	17,164,539	801	18 (7)
An. quadriannulatus	538	1,846,441	74	10,289	294	5,492,301	206	244 (0)
An. sinensis	2,944	109,624	7	10,962	1,325	293,848	20	1,619 (478)
An. stephensi	473	851,727	44	10,028	204	2,772,062	131	269 (0)
All species	36,634	1,272,063	37	183,680	13,567	3,261,557	94	23,068 (3,126)

Species name	Genome assemblies before ADseq				Genome scaffolds after ADseq **(Whole Genome topology)**			
	contigs with gene				scaffolds with gene			
	#CTG	N50		#gene	#scaffolds	N50		#new adj (#scaff adj)
		bp	#gene			bp	#gene	
An. albimanus	49	18,068,499	916	9,056	47	18,068,499	916	2 (2)
An. arabiensis	273	5,830 121	321	10,298	214	9,972,103	464	59 (14)
An. atroparvus	345	9,206,694	512	10,400	307	10,083,987	647	38 (12)
An. christyi	4,731	17,384	2	8,792	1,408	93,948	12	3,323 (207)
An. culicifacies	4,912	34,064	3	11,213	1,338	208,611	19	3,575 (1,363)
An. darlingi	1,951	118,843	9	8,617	1,265	197,190	14	686 (NA)
An. dirus	231	7,656,907	406	9,883	176	17,377,229	778	55 (10)
An. epiroticus	963	425,117	24	9,855	368	1,662,136	78	595 (7)
An. farauti	349	1,235,781	64	10,239	170	2,391,621	146	179 (63)
An. funestus	562	703,988	36	10,077	232	2,673,183	127	330 (112)
An. gambiae	6	49,364,325	2,339	10,324	6	49,364,325	2,339	0 (NA)
An. maculatus	9,473	5,042	1	10,552	3,023	31,226	7	6,450 (297)
An. melas	7,723	21,730	2	12,567	2,643	94,004	9	5,080 (162)
An. merus	997	400,239	23	10,736	406	1,260,898	65	591 (399)
An. minimus	114	10,313,149	682	9,792	96	17,164,539	801	18 (7)
An. quadriannulatus	538	1,846,441	74	10,289	297	4,868,888	206	241 (0)
An. sinensis	2,944	109,624	7	10,962	1,325	297,247	19	1,619 (475)
An. stephensi	473	851,727	44	10,028	204	2,792,811	131	269 (0)
All species	36,634	1,272,063	37	183,680	13,525	3,261,557	94	23,110 (3,130)

Table 5 Scaffolding statistics on the 18 Anopheles genomes before and after ADseq (with the X (upper table) and WG (lower table) species phylogenies). The columns 2-5 correspond to assemblies statistics before running the ADseq algorithm. Column 2 corresponds to the number of contigs in reference assemblies. The N50 statistic corresponding to the contig size where 50% of the total assembly length is comprised in contigs with size superior or equal to this value. This metric is computed with size considerd both in bp (in column 3) and in gene number (in column 4). Column 5 gives the number of genes in genome assemblies give as input to ADseq. Columns 6-9 and 10-13 represent scaffolding statistics of ADseq respectively for X chromosome species tree topology and Whole-Genome topology. Columns 6 & 10 represent scaffolds number after ADseq. Columns 7 & 11, and 8 & 12 represent N50 statistics respectively for size in bp and size in gene number. Columns 9 & 13 represent new adjacencies inferred by ADseq (#scaff adj) represent the number of new adjacencies that are scaffolding adjacencies (i.e. adjacencies with sequence signal proposed by BESST and inferred by ADseq).